

Response to review for gmd-2014-182

Dear Guy Munhoven,

Please find the detailed response to the comments from the two reviewers below (in blue). The most significant change to the manuscript was that I extended the spin-up by 2500 years, as was requested by both reviewers. I then re-did all figures and re-calculated all numbers in the manuscript based on the new simulations started from the end of this extended spin-up, but this resulted in very small changes only, and did not change any of the conclusions. Other minor changes to the text were made to address the comments from the reviewers, as you can see in the answers below and in the marked up version of the manuscript.

I hope you will find the revised manuscript acceptable for publication in GMD.

Best regards,
Alexandra Jahn

Author comment, reply to Reviewer #1

[We thank the reviewer for his/her time and for the constructive comments, which helped us to improve the manuscript. In the following, we have addressed all comments.](#)

This article describes the implementation of ^{14}C and ^{13}C into the ocean component of CESM1. ^{14}C is implemented in two different ways: an “abiotic” version following OCMIP-2 protocol that can be run without the ecosystem model, and the full “biotic” version. ^{13}C is implemented with three different options for fractionation parameterizations during photosynthesis. I have found this paper well written and suitable for GMD after major revisions as outlined below.

[We thank the reviewer for his/her positive evaluation of the manuscript.](#)

Major comments

One major concern is that the model simulations presented here are not in equilibrium yet (especially ^{14}C in the biotic configuration is far from being equilibrated). It is therefore hard to assess the model’s performance when comparing simulated fields with observations. While this is accepted (although not ideal) for high-resolution models when one is interested in temperature or salinity fields, it gets trickier with carbon-related parameters. DIC and ^{13}C in the deep ocean will take over 5,000 years to equilibrate while ^{14}C needs at least 10,000. There are models in the literature with comparable resolution, which have shown equilibrated carbon isotope fields. Given that this manuscript is a model description as well as a validation of the implemented new schemes, I fell uneasy with the model-data comparison as it stands. I am not sure what the options are at this point. I guess that by the time this paper went through the first round of review, the model had time to

run for at least another 2,000 to 4,000 years. Otherwise it might be wise to wait for Keith Lindsay's fast spin-up technique before resubmitting.

Following the reviewer's suggestion, we have completed another 2450 years of spin-up over the last few months, for a total spin-up of 6010 years before the transient simulations from 1765 to 2007. After this longer spin-up, the percentage of the ocean that is spun-up to the OCMIP2 criteria of a drift of less than 0.001%/year for the biotic radiocarbon increased from 5% to 26%, while it did not change the ^{13}C state by much. Several thousand years more would likely be required to fully spin-up the biotic radiocarbon, based on the experience from the abiotic radiocarbon. However, we do not have the computational or personal resources to do this, and the fast spin-up technique for the ecosystem model is not ready at this point. Furthermore, the 3 degree model forced by normal year forcing is not the model version this is used for science applications, so we plan to validate the carbon isotope simulation in the fully coupled CESM at 1 degree resolution in the future before any scientific applications, as mentioned at the end of the manuscript in the summary. Nevertheless, we have updated all the figures and numbers in the manuscript after the extended spin-up. The changes are very small, however, suggesting that the comparisons with the observations are not strongly affected by the continued spin-up, as most of the change is occurring in the deep ocean.

In regards to the reviewers comment that other models having shown more spun-up conditions we would like to note that to our knowledge, no other model has previously included a biotic radiocarbon tracer in their simulation. The ^{13}C and abiotic radiocarbon on the other hand, which have been included in other models before, are sufficiently spun-up in our simulation, similar to other models. We hope that the editor and the reviewers agree that publishing the paper after the extended spin-up (6000 years) carries value for the community, especially given that this is mainly a technical model documentation paper.

Once the model is in equilibrium, I would suggest showing Taylor diagrams for ^{13}C and ^{14}C for each ocean basin (in addition to the figures that are included in this first version) to quantify how well CESM1 is doing in comparison to observations/reanalysis and maybe even in comparison to one or two other isotope-enabled models (MoBidiC, PISCES, CM2Mc ESM, HAMOCC2s, UVic ESCM).} In terms of comparing to other models, we would like to note that this paper is not meant to be a model intercomparison paper, but a technical paper that describes and documents a new model feature, which is why it was submitted to GMD. And while we hope to participate in and potentially lead a model intercomparison of carbon isotope enabled models in the future, as we agree that it would be very valuable, it is far beyond the scope of this paper to obtain the results from other models and analyze them. In addition, we would use the higher resolution CESM for such a paper, as the 3 degree model version is mainly used for model development, rather than science applications.

We have also carefully considered the reviewers suggestion to using a Taylor diagram in addition to the existing plots. However, due to the sparse data coverage (in time and space), together with the coarse model grid we have decided that it is

not very useful, and potentially misleading, to compare the model and data in a Taylor diagram. We intent to use Taylor diagrams for future comparisons with other carbon isotope enabled models, and will include the available observations at that point as well, as reference, but with the caution that it is based on very sparse point-data coverage (for ^{13}C) for different seasons and years and/or globally mapped data (for ^{14}C) that is extrapolated in time and space, which can bias the comparisons.

Page 7466, lines 6/7 “The error in D14C due to neglecting biology activity has been estimated to be on the order of 10\% (Fiadiero, 1982)”. This is an interesting statement that could actually be tested with this new version of CESM1 if it was run into equilibrium.

We agree, and we plan to do this once we have a fast spin-up technique that will allow us to spin-up both the biotic and abiotic radiocarbon to equilibrium. However, as we note on page 7478 of the original manuscript, this will be the topic of a future study. We have now added an additional sentence in the manuscript that refers to these plans.

Page 7477, lines 20-24: is there a reason (other than for removing the drift) that repeated climatological forcing has been used for the simulations over the 20th century? I think that changes in ocean forcing should be included if one wants to compare ^{14}C and ^{13}C with present day data. If the authors decide to follow my suggestion above and present preindustrial results that are in (quasi) equilibrium, no drift will need to be removed and they will be able to run a more realistic transient simulation over the 20th century.

The reason for using the normal-year forcing is that the physical model state has been spun-up for over 6000 years using the normal-year forcing. Switching to the interannual CORE forcing (available for 1948-2007) creates large drifts in the model state, and the discontinuity between repeating cycles of this 60-year forcing leads to repeated adjustment periods (with large shocks to the system) that last at least 10 years (see the many CORE and CORE2 papers that use this forcing and describe its effect, at <http://www.clivar.org/clivar-panels/omdp/core-2>). For the purpose of this paper, we prefer to use the climatological forcing, which does not introduce any such additional drifts and discontinuities. The fact that the radiocarbon inventory and the Suess effect can be simulated relatively well despite the use of the climatological forcing suggests that changing temperature and/or winds over the 20th century are not the main drivers of these observed changes, but that the large changes in the atmospheric concentrations dominates these effects, as would be expected.

We have now made it clearer in the revised manuscript why we use the climatological forcing, by including the statement below: “We chose to continue with the climatological CORE-II forcing rather than use the interannually varying CORE-II forcing for 1948-2007 in order to avoid shocks to the ocean when switching the forcing and when the forcing jumps from 2007 back to 1948 every 60 years, which impacts the simulation for 10 years or more (Danabasoglu et. al., 2014), and would overlap with the start of the introduction of bomb radiocarbon into the atmosphere.”

Overall, the paper is quite descriptive and in some places lacks analysis. For example: Page 7482, lines 15-18, why are 13C DIC values smaller than observed? Is that an artefact of the physical circulation? Or is the remineralization depth not very well represented? See also lines 21-23. Figure 2, why are the surface subtropics older than observations in the biotic simulation? Why is the deep Pacific not ventilated enough? How do AABW formation rates compare with observations? Where are the convection sites?

We have added a bit more explanations of some of these biases in the revised manuscript. In particular, we have added the following to the end of the sentence about the deep Pacific not being ventilated enough, which also refers to the AABW: “and is related to too weak Antarctic Bottom Water formation in the CESM (Danabasoglu et. al. 2011) and too shallow mixed layers in the Southern Ocean (Moore et. al. 2013). “. But since this model version used here (3 degree, climatological forcing) is not the model version commonly used for science application, an in depth analysis of the causes of some of these biases is beyond the scope of this paper and would not be very useful for future users, as the biases might look different in the fully coupled CESM. As mentioned at the end of the manuscript, we intend to perform a more in-depth validation in the newest version of the fully coupled CESM at 1 degree resolution before using the carbon isotopes for science applications in the future.

Page 7485, lines7-14: can you please provide more details about the sediment model? Especially with regards to 14C? Does the sediment model keep track of 14C in calcite between deposition and dissolution?

We have decided to remove the section on the changes to the carbon isotopes in the CESM1.2, as it was decided (not by us, but the CESM steering group) since we originally submitted the manuscript that there would be no release of the CESM in 2015. This means that the carbon isotopes will therefore only be publically released as part of the CESM2 release in 2016, which will have further significant changes compared to the CESM1.0.5 shown here (and the CESM1.2 version described in the GMD discussion paper). This makes the inclusion of this section obsolete, as there will be no public release of the carbon isotope code with the changes described here for the CESM1.2, and this paper used the CESM1.0.5. Instead of this section, we will include the carbon isotope code for the CESM1.0.5 (as used for this manuscript) as supplementary material with the revised manuscript.

To answer the reviewer’s question, there actually is no full sediment model in the ocean ecosystem model in the CESM1.2, and we regret if we created the impression that there was one. Instead, ocean sedimentation is parameterized by including a new burial term. This burial term is very idealized, and once carbon is buried it is no longer tracked, so no dissolution of calcite is accounted for. Improvements to the treatment of burial are ongoing, and will be documented for the CESM2, at which time we will include a description in the model documentation on how the carbon isotopes are handled.

Minor comments

Page 7466, lines 23/26; by using the daily mean of the squared 10m wind speed instead of squared monthly average plus variance you might resolve storms more accurately. This might lead to an overestimation of the air-sea gas exchange with parameters tuned to monthly means and might explain the relatively high simulated excess radiocarbon inventory (page 7479). This is just a comment, I do not expect the authors to change their air-sea gas exchange parameterisation.

We agree that this might be the case, but have not changed the air-sea gas exchange parameterization, as it is the standard air-sea gas exchange parameterization used in the CESM.

Page 7467, line 10: should the unit of Alkbar be in mol/kg? Or in eq/kg?}

Thank you for catching this, the unit of Alkbar should be in microeq/kg and this has been changed in the manuscript.

Page 7468, equation 4: PV scales with $Sc^{(-1/2)}$ not $Sc^{(1/2)}$

Equation 4 does show PV scaling correctly with $Sc^{(-1/2)}$, so we are not sure what the reviewer means here. Consequently, no change was made.

Page 7468, line 12: is * defined somewhere?}

It was not defined by mistake. We define it now after it is first used: “ ΔCO_2^* being the difference in CO_2 concentration between the surface ocean and the atmosphere”

Page 7480, line 11: this number is meaningless if the model is not in equilibrium (natural radiocarbon inventory before anthropogenic disturbances).

We agree that the biotic model might still not be at its final radiocarbon inventory due to the continuing spin-up, and have added a qualifier here (see below):

“However, the biotic model estimate of the natural radiocarbon inventory might still not be the final value, as the biotic radiocarbon is still spinning-up. In terms of the anthropogenic radiocarbon inventories presented next, this biases should not play any large role, however, as we remove any remaining drift.”

Page 7484, line 5: “-0.018 per mil per decade (Gruber et al 1999)” should be -0.18 per mil per decade (it is reported in the original Gruber paper as 0.018 per year). }

Thank you for finding this error, it has been corrected and it now reads “-0.18 per mil per decade”

Page 7494, table caption: one “based on” to many.

Thank you for finding this typo, it has been fixed and it now reads “are based on”

Author comment, reply to Reviewer #2

We thank the reviewer for his/her time and for the very detailed and constructive comments, which helped us to improve the manuscript. In the following, we have addressed all comments.

The manuscript by Jahn et al. describes a new implementation of the carbon isotopes ^{14}C and ^{13}C into the ocean component of the Community Earth System Model (CESM1). ^{14}C and ^{13}C are tracers that are often used as paleoclimatological proxies, but that can also be used e.g. as proxies of anthropogenic carbon or to validate the ventilation of the deep ocean in circulation models. Two different implementations are described: One that models only ^{14}C and neglects biological

uptake following the OCMIP-2 protocol, and one that models both ^{14}C and ^{13}C and that takes into account fractionation during biological formation of particulate carbon (both organic and calcium carbonate). After a detailed and useful description of the implementation in chapter 3, it demonstrates the use of the implemented carbon isotopes by comparing them to present-day ocean observations in chapter 4. One interesting aspect of the paper is that several formulations for the fractionation during phytoplankton growth that have been discussed in the biological literature are implemented here, so that one can see whether they result in very different distributions of ^{13}C in the ocean. The effect is relatively minor, which is reassuring for people using carbon isotopes as proxies.

We thank the reviewer for his/her positive evaluation of the manuscript.

Major comments

What is lacking in the manuscript is a brief overview over where the implementation differs from that in other models, e.g. those cited on page 7463. This could easily be amended.

As suggested, we have now included a short statement in the introduction where the other models that include carbon isotopes are mentioned, and also added a discussion of how the model differs in other places in the manuscript (e.g. in the discussion of the fractionation during the formation of calcium carbonate).

The description of the model implementation of the carbon isotopes, which is the main focus of the paper, is detailed and well-written, and it will become a useful reference for other groups that want to include isotopes into their ocean biogeochemical models. I would therefore recommend to accept the paper for publication after a few minor revisions.

I share the concern by the first reviewer that the model runs presented in the results section are not in equilibrium, especially the distribution of ^{14}C in the biotic run. Probably, in the meantime the model has run for a few thousand model years longer and I would suggest to replace the figures and numbers in the results section with ones from a later stage of the model experiments.

We have now run the model for another 2450 years, for a total spin-up of 6010 years, and have updated the text and all figures accordingly (with very little changes in the figures and only small changes in some numbers that did not change any conclusions or comparisons with the observations). While the biotic radiocarbon is still not fully spun-up, it is now at 26% compared to 5% for the OCMIP2 criteria, which is very strict. The ^{13}C and DIC did not change much during the continued spin-up, so we consider these spun-up, and a shorter spin-up of 3000 years or less seems sufficient for these tracers. As the main purpose of this article is to document the implementation, we think that this is good enough for now. We look forward to eventually having a fast spin-up technique available that will allow us to use the biotic radiocarbon for science applications beyond the documentation of the model.

The authors use a constant fractionation of 2‰ for ^{13}C during formation of calcium carbonate, referring to Ziveri et al. (2003) (page 7474). Ziveri shows a range of about 5‰ for different species (from +3 to -2), and several other studies indicate a smaller fractionation around 1‰, see e.g. Zeebe and Wolf-Gladrow (2001), Figure 3.2.13. Although the effect on ^{13}C in dissolved inorganic carbon is probably negligible, this may bias the interpretation of ^{13}C values from marine carbonates. I would suggest that the authors describe briefly the range of fractionation factors found and add a few more citations.

We have expanded this paragraph to mention what other model implementations have used as well as give the range of the values reported by Ziveri et al. See below for the revised text.

“While the fractionation during calcium carbonate formation is much smaller than the fractionation during photosynthesis (Turner, 1982), we include a small constant fractionation of 2‰ for calcium carbonate formation, based on work by Ziveri et al. (2003) that found a range of 3‰ to -2‰ for different species. Other implementations of ^{13}C in ocean models have used values of 1‰ (e.g., Sonnerup et al. 1999, Alessandro & Bopp 2008) or have assumed no isotopic fractionation for calcification (e.g., Marchal et al 1998, Schmittner et al. 2013). However, the effect of the calcium carbonate pump on $\delta^{13}\text{C}$ is small as was shown by Schmittner et al. (2013), so the choice of the value for the fractionation during calcium carbonate formation is not expected to have a big impact on the results in the current ecosystem model with one species of calcium carbonate.”

Chapter 5 describes very briefly that the carbon isotopes have now also been implemented in CESM version 1.2, which includes a simple description of marine sediments. How this sediment model works, however, is not described in sufficient detail, and neither is how the carbon isotopes are represented in it. Early diagenesis can affect the isotopic composition of DIC near the bottom of the ocean and of foraminifera recording it (Mackensen et al., 1993), and it would be useful to know whether these effects are represented in the model. I would therefore suggest that the authors add a little more model description here. Are the modeled distributions of carbon isotopes in the water column affected to some extent by the addition of a sediment module, e.g. by a burial loss with a ^{13}C that differs from the average ^{13}C of seawater?

As mentioned in the reply to reviewer 1, we have decided to remove the discussion of the changes to the carbon isotopes in the CESM1.2, as the CESM has continued to evolve since we submitted this paper (including how the sedimentation is parameterized), and there will be no release of the CESM1.3 in 2015 after all. This means that the carbon isotopes will therefore only be included in the CESM2 release in 2016, which will have yet further changes compared to the CESM1.0.5 shown here, making the discussion of the changes in the CESM1.2 obsolete. Once the CESM2 code is finalized we will include a description of how the carbon isotopes are included in that version in the description of that model. In the meantime, we will

include the carbon isotope code as used here (in version CESM1.0.5) with the revised manuscript.

Minor comments

Page 7478, line 18: 'differences . . . is': either use singular or plural

Thank you for finding this error, it has been corrected to "differences are"

Page 7492, line 28: 'active uptake or' ! 'active uptake of'

Thank you for finding this error, it has been corrected to "active uptake of"

Page 7494, caption table 1: 'using' ! 'used'

Thank you for finding this error., it has been corrected to "Parameters used ..."

Carbon isotopes in the ocean model of the Community Earth System Model (CESM1)

Alexandra Jahn^{1*}, Keith Lindsay¹, Xavier Giraud^{2,3}, Nicolas Gruber³, Bette L. Otto-Bliesner¹, Zhengyu Liu⁴, and Esther C. Brady¹

¹National Center for Atmospheric Research, Climate and Global Dynamics Division, Boulder, CO, USA

²Aix Marseille Université, CNRS, IRD, Collège de France, CEREGE UM34, Aix en Provence, France

³Environmental Physics Group, Institute of Biogeochemistry and Pollutant Dynamics, ETH Zürich, Zürich, Switzerland

⁴Department of Atmospheric and Oceanic Sciences, and Center for Climatic Research, University of Wisconsin – Madison, Madison, WI, USA

*Now at the Department of Atmospheric and Oceanic Sciences and the Institute of Arctic and Alpine Research at the University of Colorado Boulder, Boulder, CO, USA

Correspondence to: Alexandra Jahn
(alexandra.jahn@colorado.edu)

Abstract.

Carbon isotopes in the ocean are frequently used as paleo climate proxies and as present-day geochemical ocean tracers. In order to allow a more direct comparison of climate model results with this large and currently underutilized dataset, we added a carbon isotope module to the ocean model of the Community Earth System Model (CESM), containing the cycling of the stable isotope ¹³C and the radioactive isotope ¹⁴C. We implemented the ¹⁴C tracer in two ways: in the “abiotic” case, the ¹⁴C tracer is only subject to air–sea gas exchange, physical transport, and radioactive decay, while in the “biotic” version, the ¹⁴C additionally follows the ¹³C tracer through all biogeochemical and ecological processes. Thus, the abiotic ¹⁴C tracer can be run without the ecosystem module, requiring significantly less computational resources. The carbon isotope module calculates the carbon isotopic fractionation during gas exchange, photosynthesis, and calcium carbonate formation, while any subsequent biological process such as remineralization as well as any external inputs are assumed to occur without fractionation. Given the uncertainty associated with the biological fractionation during photosynthesis, we implemented and tested three parameterizations of different complexity. Compared to present-day observations, the model is able to simulate the oceanic ¹⁴C bomb uptake and the ¹³C Suess effect reasonably well compared to observations and other model studies. ~~At the same time, the carbon isotopes reveal biases in the physical model, for example a too sluggish ventilation of the deep Pacific Ocean.~~

1 Introduction

20 A large fraction of paleoclimatic reconstructions are based on isotopic measurements (e.g. Petit et al.,
1999; McDermott, 2004; Curry and Oppo, 2005; Polka et al., 2013), yet there are many uncertainties
associated with the interpretation of these records in terms of physical climate variables such as
temperature, precipitation, and ocean circulation rates. More direct comparisons of paleo data with
climate models would therefore be beneficial, both to test the interpretation of the isotopic proxy
25 data and to allow for better comparisons of model simulations with proxy data. Furthermore, many
isotope tracers are currently being measured in the ocean, and including them in ocean models can
help us better understand the ocean circulation and diagnose model biases (e.g. Matsumoto et al.,
2004). For all of these reasons, we have added a carbon isotope module to the ocean model of the
Community Earth System Model (CESM) (Hurrell et al., 2013).

30 Carbon has two stable isotopes, ^{12}C and ^{13}C . More than 98.9% of carbon on earth is ^{12}C ,
while ^{13}C makes up most of the remaining 1%. The radioactive carbon isotope ^{14}C , also called
radiocarbon, is present only in trace amounts (approximately $1 \times 10^{-10}\%$ of all carbon) and has
a half-life of 5730 years (Godwin, 1962). Radiocarbon is a useful tracer to evaluate the ventilation
of the deep ocean because it acts as a clock, measuring the time since water was last in contact with
35 the atmosphere (e.g. Toggweiler et al., 1989; Orr, 2002; Meissner et al., 2003; Waugh et al., 2003;
Key et al., 2004; Doney et al., 2004; Matsumoto et al., 2004; Meissner, 2007; Bardin et al., 2014).
Because of the atmospheric nuclear weapons tests in the 1950s and 1960s and the well-known input-
function of radiocarbon during this time, radiocarbon is also useful to evaluate the recent penetration
of anthropogenic carbon into the ocean (e.g. Graven et al., 2012). Furthermore, oceanic radiocarbon
40 has been used to determine the mean gas exchange velocity used in ocean models (e.g. Wanninkhof,
1992; Sweeney et al., 2007; Naegler et al., 2006; Naegler, 2009). Oceanic $\delta^{13}\text{C}$ has been used in
paleoclimate studies as a tracer of the ocean circulation (e.g. Marchal et al., 1998; Curry and Oppo,
2005; Crucifix, 2005), to calculate the uptake of anthropogenic carbon dioxide (e.g. Keeling et al.,
1980; Quay et al., 1992; Gruber et al., 1999; Sonnerup et al., 1999; Gruber and Keeling, 2001), and
45 to diagnose biases in marine ecosystem models (e.g. Schmittner et al., 2013).

We added the carbon isotopes to the code [in a way so](#) that they follow the cycling of total carbon
through all ecosystem and physical/chemical processes. In this biotic formulation, a new ^{13}C and
 ^{14}C state variable was added to each carbon-bearing state variable resulting in a total of 14 new state
variables. For ^{14}C , we also added the option of a simplified representation, where the isotope is only
50 subject to the main chemical and physical processes during gas exchange and decay, but does not
cycle through the ecosystem. This abiotic formulation of ^{14}C was implemented based on the Ocean
Carbon Model Intercomparison Project Phase 2 (OCMIP-2) protocol (Orr et al., 2000).

Abiotic radiocarbon had been added previously to the NCAR ocean model (in NCOM1.4, Orr,
2002, and POP1/CCSM3, Graven et al., 2012), and biotic ^{13}C was implemented into the ecosystem
55 model of the CCSM3 by X. Giraud and N. Gruber in 2009–2010. However, neither development was

ever added to the trunk of the ocean model code of the CESM, so it was not maintained as the model evolved over the years and consequently none of these implementations still work in the current ocean model of the CESM. ~~The current developments have been added to the code trunk of the current ocean model of CESM.~~ In contrast, the addition of a biotic radiocarbon tracer is completely new in this implementation in the CESM. In order to increase the chances of maintaining these developments as the model continues to evolve, the current implementation has been added to the code trunk of the current ocean model of CESM. By including carbon isotopes in the ocean model of the CESM1, the CESM1 joins the community of other comprehensive ocean general circulation models that include abiotic radiocarbon and/or biotic ^{13}C in the ocean (e.g. MoBidiC, Crucifix, 60 2005, PISCES, Tagliabue and Bopp, 2008, CM2Mc ESM, Galbraith et al., 2011, HAMOCC2s, Hesse et al., 2011, and UVic ESCM, e.g. Meissner et al., 2003; Schmittner et al., 2013). While the abiotic radiocarbon implementation tends to follow the OCMIP-2 protocol (Orr et al., 2000) in all models, the implementations of biotic ^{13}C differs between models, mainly due to the complexity of the ocean biogeochemistry model used in them, but also due to different choices in regards to 70 the parameterization of the biological fractionation during photosynthesis and calcium carbonate formation.

As a reference for future studies using these new capabilities in the CESM, we describe the model used (Sect. 2), describe the details of the implementation of the abiotic and biotic carbon isotopes (Sect. 3), and compare the simulated carbon isotope fields to observational data to show the general performance of the model (Sect. 4). ~~and mention changes in the most recent version of the CESM as they relate to the carbon isotopes (Sect. ??).~~

2 Model

This work was done using the Community Earth System Model (CESM) (Hurrell et al., 2013), ~~versions version~~ 1.0.5. It has been ~~adapted to CESM1.2 (see Sect. ??)~~ updated to the current version 80 of the CESM and is targeted for public release in ~~2015-2016~~ as part of ~~CESM1.3~~ CESM2 (see the section on code availability at the end of the article). The CESM is a fully-coupled climate model with components for the atmosphere, land, river runoff, sea ice, ocean and ice sheets, coupled by a coupler. Its components and simulations have been described in a large collection of articles, many of them contained in a special collection in the Journal of Climate (<http://journals.ametsoc.org/page/CCSM4/CESM1>). The simulations analyzed here were performed using the ocean model coupled to data models for the atmosphere, the land, the sea ice, and the river routing, using repeated normal 85 year forcing from CORE-II (Large and Yeager, 2009). The ocean model was run at a nominal 3° horizontal resolution with 60 vertical levels, which is the low-resolution configuration of the ocean model (Shields et al., 2012).

90 3 Carbon isotope implementation

The carbon isotopes were added as optional passive tracers, with the biotic and abiotic implementations as two different options that can be set at the compilation and build time. The abiotic ^{14}C can be run with or without the ocean ecosystem model, while the biotic ^{13}C and ^{14}C require the ocean ecosystem model to be turned on.

95 3.1 Abiotic ^{14}C

In this implementation, DI^{14}C is the model's normalized concentration of total dissolved inorganic ^{14}C , following the OCMIP2 protocol (Orr et al., 2000). DI^{14}C is used as normalized concentration in order to minimize the numerical error of carrying very small numbers. The normalization is done by dividing the real DI^{14}C by the standard ratio of $^{14}\text{C}/^{12}\text{C}=1.176 \times 10^{-12}$ (Karlen et al.,
100 1968). To obtain comparable DI^{14}C values as measured, we multiply the simulated DI^{14}C by this scaling factor of 1.176×10^{-12} . Since the abiotic radiocarbon is designed to be run without the ocean ecosystem active, we also carry an abiotic DI^{12}C tracer to calculate the isotope ratio $^{14}R = \text{DI}^{14}\text{C}/\text{DI}^{12}\text{C}$. For comparisons with observations, we calculate $\Delta^{14}\text{C}$ as a diagnostic variable:

$$\Delta^{14}\text{C}=(^{14}R-1) \cdot 1000. \quad (1)$$

105 By construction, the abiotic DI^{12}C and DI^{14}C tracers only depend on the solubility of carbon in seawater and neglect all biological activity. The error in $\Delta^{14}\text{C}$ due to neglecting biology activity has been estimated to be on the order of 10 % (Fiadiero, 1982).

Note that we do not multiply ^{14}R by $^{14}R_{\text{std}}$ in Eq. (1), as we are using a normalized DI^{14}C (following Orr et al., 2000). Given that this abiotic implementation does not account for the fractionation during gas exchange, we do not apply the correction for fractionation that is commonly applied to
110 observational measurements of $^{14}\text{C}/^{12}\text{C}$ ratios (as well as for the biotic ^{14}C implementation, see Eq. (27) in Sect. 3.2.4). The simulated abiotic $\Delta^{14}\text{C}$ is therefore directly comparable to observed data reported as $\Delta^{14}\text{C}$ (see Toggweiler et al., 1989, for more details).

3.1.1 Surface fluxes

115 We follow the abiotic OCMIP-2 protocol (Orr et al., 2000) for most of the implementation of the abiotic radiocarbon surface fluxes, with the following notable differences:

- We use a coefficient a of 0.31 cm h^{-1} (Wanninkhof, 1992) instead of 0.337 cm h^{-1} as used in OCMIP-2. This is higher than what most recent estimates suggest (e.g., Sweeney et al., 2007; Naegler et al., 2006; Naegler, 2009; Graven et al., 2012), but makes it consistent with
120 the gas-transfer formulation used in other parts of the CESM.
- We use the daily mean of the squared 10 m windspeed (either from the prescribed CORE-II forcing or from the coupled atmospheric model) instead of the climatology of the squared

monthly average of the instantaneous SSMI velocity and its instantaneous variance as used in OCMIP-2.

125 – We use the daily mean of the ice fraction and atmospheric pressure (either from the data models or the coupled sea ice and atmosphere models) instead of the monthly averaged climatology used in OCMIP-2.

– We use a constant reference value ($1944 \mu\text{mol m}^{-3}$) for the virtual fluxes of abiotic radiocarbon, rather than an annually updated average of the surface DI^{14}C as suggested in OCMIP-2.

130 This is done to conserve total ^{14}C in the model (in absence of radioactive decay).

To compute the partial pressure of CO_2 from the abiotic DI^{12}C , we require an estimate of surface alkalinity. We follow again OCMIP-2, i.e., we estimate surface alkalinity (Alk) by scaling the ocean mean alkalinity, $\text{Alkbar} = 2310 \text{ microeq kg}^{-1}$ with sea-surface salinity, SSS, i.e.,

$$\text{Alk} = \text{Alkbar} \cdot \rho_{\text{sw}} \cdot \text{SSS} / S_{\text{Ref}} \quad (2)$$

135 with $S_{\text{Ref}} = 34.7$ and $\rho_{\text{sw}} = 4.1/3.996 \text{ g cm}^{-3}$ (these two are constants in the CESM). We alter this calculation in the Baltic Sea and the Black Sea to avoid unrealistic Alkalinity values, following the procedure developed by K. Lindsay for creating initial conditions for the marine ecosystem model: in the Black Sea, the surface alkalinity is independent of SSS: $\text{alkalinity} = 3300 \cdot \rho_{\text{sw}}$. In the Baltic Sea, we calculate Alkalinity depending on the surface salinity, with $\text{Alkalinity} = 119 + 196 \cdot \text{SSS}$ 140 when SSS is equal to or below 7.3, and $\text{Alkalinity} = 1237 + 43 \cdot \text{SSS}$ when the SSS is above 7.3. The computation of $p\text{CO}_2$ also requires an assumption about the surface ocean concentrations of silicic acid and phosphate, for which we use OCMIP-2's global constants, i.e., $7.5 \mu\text{mol kg}^{-1}$ for silicic acid, $\text{Si}(\text{OH})_4$, and $0.5 \mu\text{mol kg}^{-1}$ for phosphate, PO_4 .

Air-sea gas exchange

145 As in OCMIP-2, the air-sea gas exchange flux of ^{12}C is calculated as

$$F = \text{PV} \cdot (C_{\text{sat}} - C_{\text{surf}}) \quad (3)$$

with PV being the CO_2 gas transfer velocity (called the piston velocity) in ms^{-1} , calculated as

$$\text{PV} = (1 - \text{aice}) \cdot a \cdot u_{10}^2 \cdot (660.0 / Sc_{\text{CO}_2})^{-1/2}. \quad (4)$$

The coefficient a is taken as 0.31 cm h^{-1} as mentioned earlier, aice is the fraction of the ocean 150 covered by sea ice, u_{10}^2 is the squared 10 m wind speed from the coupler, and Sc_{CO_2} is the Schmidt number of CO_2 . Sc_{CO_2} is calculated as in the ecosystem model, following Wanninkhof (1992):

$$Sc_{\text{CO}_2} = 2073.1 + \text{SST} \cdot (-125.62 + \text{SST} \cdot (3.6276 + \text{SST} \cdot (-0.043219))). \quad (5)$$

C_{surf} in the gas flux calculation above is the surface aqueous CO_2 concentration in mol m^{-3} (also called CO_2^* , which is the aqueous CO_2 concentration in mol m^{-3} in the ocean in general). C_{sat} is the saturation concentration in mol m^{-3} , with $C_{\text{sat}} = \text{CO}_2^* + \text{DCO}_2^*$, ~~and~~ and DCO_2^* being the difference in CO_2 concentration between the surface ocean and the atmosphere. SST is the sea surface temperature. CO_2^* and DCO_2^* in turn are calculated by the carbonate solver from the ecosystem model, based on SST, SSS, ALK, PO_4 , $\text{Si}(\text{OH})_4$, pH, atmospheric $p\text{CO}_2$, atmospheric pressure, and the abiotic DI^{12}C and DI^{14}C concentration in the surface water.

160 As in OCMIP-2, we do not account for fractionation during gas exchange in this abiotic formulation, as the effect of isotopic fractionation is almost completely accounted for by the standard correction made when calculating $\Delta^{14}\text{C}$ from observations (see Toggweiler et al., 1989, for details).

The gas flux of the normalized abiotic DI^{14}C is calculated as

$$F^{14} = PV \cdot (C_{\text{sat}} \cdot R^{14}\text{C}_{\text{atm}} - C_{\text{surf}} \cdot R^{14}\text{C}_{\text{ocn}}) \quad (6)$$

165 with

$$R^{14}\text{C}_{\text{atm}} = (1 + \Delta^{14}\text{C}_{\text{atm}}/1000) \quad (7)$$

and

$$R^{14}\text{C}_{\text{ocn}} = 1000 \cdot (\text{DI}^{14}\text{C}/\text{DI}^{12}\text{C} - 1). \quad (8)$$

170 The values of the atmospheric $p\text{CO}_2$ and $\Delta^{14}\text{C}_{\text{atm}}$ can be set to be constants or can be read in from a file. For atmospheric $p\text{CO}_2$, it can also be taken from the coupler, to ensure the use of a consistent atmospheric $p\text{CO}_2$ value across model components. Currently the code is set up to read in three files of $\Delta^{14}\text{C}_{\text{atm}}$ values, one each for the Northern Hemisphere, the equatorial region (20°N – 20°S), and the Southern Hemisphere, in order to represent the spatial inhomogeneity of $\Delta^{14}\text{C}_{\text{atm}}$, for example after the atmospheric nuclear bomb tests.

175 **Virtual fluxes**

The CESM ocean model is a volume-conserving model where water fluxes at the surface (from precipitation, evaporation, and river input) are added as virtual fluxes. These virtual fluxes represent the dilution or concentration effect from adding or removing freshwater. For the abiotic carbon isotope tracers, we have a virtual DI^{12}C and DI^{14}C flux. As for salinity and for DIC in the ecosystem model, we use a constant surface reference DI^{12}C and DI^{14}C for the calculation of virtual fluxes in order to conserve tracers. The reference values are $1944 \mu\text{mol m}^{-3}$ for both DI^{12}C and normalized DI^{14}C , the same as for DIC in the ecosystem model of CESM.

3.1.2 Interior processes

In the interior of the ocean, the only additional term to the transport of the tracers by the physical
185 ocean model is the decay term for DI^{14}C , following the OCMIP-2 protocol.

$$d[\text{DI}^{12}\text{C}]/dt=L([\text{DI}^{12}\text{C}]) \quad (9)$$

and

$$d[\text{DI}^{14}\text{C}]/dt=L([\text{DI}^{14}\text{C}])-\lambda \cdot [\text{DI}^{14}\text{C}] \quad (10)$$

with L being the 3-D transport operator and λ being the radioactive decay constant for ^{14}C in s^{-1} ,
190 using a half-life of 5730 years (Godwin, 1962):

$$\lambda = \ln(2)/(5730 \cdot 31556926). \quad (11)$$

The radiocarbon age (relative to AD 1950 = 0 yr BP) is calculated from $\Delta^{14}\text{C}$ following:

$$^{14}\text{C}_{\text{age}} = -5730/\ln 2 \times \ln(1 + \Delta^{14}\text{C}/1000) \quad (12)$$

5730 years / $\ln 2 = 8267$ years is the mean life of ^{14}C , which differs from the often used mean-life
195 of 8033 years (e.g. Stuiver and Polach, 1977), which is based on the earlier Libby half-life of 5568
(Libby, 1955).

3.2 Biotic ^{13}C and ^{14}C

In the biotic implementation of ^{13}C and ^{14}C , we use the ocean ecosystem model (e.g. Moore et al.,
2013) to compute the carbon pools as well as all other biological variables (like silicic acid, alka-
200 linity, etc). The ecosystem model currently has seven carbon pools: DIC, DOC (dissolved organic
carbon), CaCO_3 , diazotrophs, diatoms, small phytoplankton, and zooplankton. We carry passive
tracers for each of these in the isotope-enabled version of the code. As ^{12}C makes up over 98 % of
the carbon earth and does not fractionate, we assume that the ecosystem carries ^{12}C . This means that
the isotope ratio R can be calculated as the ratio of the new isotopic carbon pools to the ecosystem
205 carbon pools. As for the abiotic radiocarbon, we use scaled variables for ^{13}C and ^{14}C in order to min-
imize the numerical error of carrying very small numbers (particularly for ^{14}C). The scaling factor is
the commonly used standard $^{13}\text{C}/^{12}\text{C}$ for each isotope, i.e., 1.12372×10^{-8} for $\text{iso} = ^{13}\text{C}$ (Craig,
1957) and 1.176×10^{-12} for $\text{iso} = ^{14}\text{C}$ (Karlen et al., 1968). This means that we use $^{13}R_{\text{Std}} = 1$
and $^{14}R_{\text{Std}} = 1$ in the code, and that the model simulated isotopic carbon pools are multiplied by the
210 respective scaling factor to compare them with observations.

In the biotic formulation, we account for the fractionation of ^{13}C and ^{14}C during gas exchange
and during biological processes. The fractionation (ϵ) of ^{14}C is always twice that of ^{13}C , as all
relevant processes have a mass-dependent fractionation for carbon (Bigeleisen, 1952; Craig, 1954).

The isotopic fractionation ϵ is related to the fractionation factor α through:

$$215 \quad \epsilon = (\alpha - 1) \cdot 1000. \quad (13)$$

As diagnostic variable, we compute the $\delta^{\text{iso}}\text{C}$ values by first computing the ratio $^{\text{iso}}R = \text{DI}^{\text{iso}}\text{C}/\text{DIC}$, and then using

$$\delta^{\text{iso}}\text{C} = (^{\text{iso}}R - 1) \cdot 1000. \quad (14)$$

As for the abiotic $\Delta^{14}\text{C}$ calculation in Eq. (1), we do not multiply by $^{\text{iso}}R_{\text{Std}}$ in the calculation of
220 $\delta^{\text{iso}}\text{C}$ because we are using normalized $\text{DI}^{\text{iso}}\text{C}$.

3.2.1 Air-sea gas exchange of ^{13}C

The air-sea flux of ^{13}C is calculated based on Zhang et al. (1995):

$$F^{13} = PV \cdot \alpha_{\text{aq}_g} \cdot \alpha_k \cdot (R^{13}\text{C}_{\text{atm}} \cdot C_{\text{sat}} - R^{13}\text{C}_{\text{DIC}} \cdot C_{\text{surf}} / \alpha_{\text{DIC}_g}). \quad (15)$$

Here, C_{sat} and C_{surf} are obtained from the ecosystem model. $\alpha_k = -0.99919$ is the constant kinetic
225 fractionation factor from Zhang et al. (1995) (with $\epsilon = -0.81$ and $\alpha = \epsilon/1000 + 1$). α_{aq_g} is the temperature (TEMP, in $^{\circ}\text{C}$) dependent isotopic fractionation factor during gas dissolution, based on the equation for ϵ_{aq_g} from Zhang et al. (1995).

$$\epsilon_{\text{aq}_g} = -0.0049 \cdot \text{TEMP} - 1.31. \quad (16)$$

The temperature and carbonate fraction (f_{CO_3}) dependent fractionation factor (α_{DIC_g}) between total
230 DIC and CO_2 is based on the empirical relationship for ϵ_{DIC_g} from Zhang et al. (1995):

$$\epsilon_{\text{DIC}_g} = 0.014 \cdot \text{TEMP} \cdot f_{\text{CO}_3} - 0.105 \cdot \text{TEMP} + 10.53. \quad (17)$$

$R^{13}\text{C}_{\text{atm}}$ is the ^{13}C to ^{12}C ratio in atmospheric CO_2 , calculated using the atmospheric $\delta^{13}\text{C}_{\text{atm}}$
record and $R_{\text{atm}} = 1 + \delta^{13}\text{C}_{\text{atm}}/1000$ (scaled by $^{13}R_{\text{Std}}$). The values of $\delta^{13}\text{C}_{\text{atm}}$ can be set to be
235 a constant or it can be read in from a file. Currently $\delta^{13}\text{C}_{\text{atm}}$ is assumed to be well mixed globally, so only one global value is read in. With small code modifications globally inhomogeneous $\delta^{13}\text{C}_{\text{atm}}$ values can easily be read in instead. $R^{13}\text{C}_{\text{DIC}}$ is the ^{13}C to ^{12}C ratio of dissolved inorganic carbon, calculated from the simulated biotic DIC and DI^{13}C .

3.2.2 Virtual fluxes of ^{13}C

As stated in Sect. 3.1.1, we account for the dilution and concentration effect of surface freshwater
240 fluxes in the model by adding a virtual flux, using a constant surface reference DI^{13}C (and DI^{14}C) of $1944 \mu\text{mol m}^{-3}$ for the calculation of virtual fluxes.

3.2.3 Biological fractionation of ^{13}C

The isotopic carbon-fixation by photosynthesis (photo ^{13}C) is computed from the ^{12}C fixation during photosynthesis (photoC, from the ecosystem model), using

$$245 \quad \text{photo}^{13}\text{C} = \text{photoC} \cdot R_p \quad (18)$$

with

$$R_p = 1000 \cdot R_{\text{CO}_2^*} / (\epsilon_p + 1000) \quad (19)$$

and

$$R_{\text{CO}_2^*} = R^{13}\text{C}_{\text{DIC}} \cdot \alpha_{\text{aq}_g} / \alpha_{\text{DIC}_g}. \quad (20)$$

250 The strength of the biological fractionation of carbon during photosynthesis (ϵ_p), as well as the key controlling parameters, are still being debated in the literature (e.g. Keller and Morel, 1999), [and many of the existing \$^{13}\text{C}\$ implementations in models use different parameterizations](#). We therefore implemented three different parameterizations for ϵ_p to test the sensitivity of our results to the choice of biological fractionation.

255 The simplest model for ϵ_p by Rau et al. (1989) gives the same ϵ_p value for all types of autotrophs:

$$\epsilon_p = 1000 \cdot (\delta_{\text{CO}_2^*} - \delta_{\text{C}_p}) / (1000 + \delta_{\text{C}_p}). \quad (21)$$

This relationship is based on the empirical relationship found by Rau et al. (1989) between the isotopic composition of the autotroph (δ_{C_p}) and CO_2^* :

$$\delta_{\text{C}_p} = -0.8 \cdot \text{CO}_2^* - 12.6, \quad (22)$$

260 limiting δ_{C_p} to values between -18 and -32‰ (Rau et al., 1989).

Laws et al. (1995) assumed that CO_2 enters the cell by diffusion and that the fractionation depends on the rate of photosynthesis, and therefore parameterized ϵ_p as a function of CO_2^* and the specific photosynthesis rate of each phytoplankton group (μ , in s^{-1} , calculated by the ecosystem model):

$$^{13}\epsilon_p = (\mu / \text{CO}_2^* \cdot 86400 - 0.371) / (-0.015). \quad (23)$$

265 Keller and Morel (1999) argued that only considering diffusive CO_2 transport into cells and assuming a linear relationship between ϵ_p and CO_2^* concentration and the specific growth rate (μ) does not agree with laboratory and field data, citing work by Sikes et al. (1980), Tortell et al. (1997), and Laws et al. (1997). Keller and Morel (1999) therefore proposed to use phytoplankton-type specific (constant) cell parameters (see Table 1) to compute the fractionation during photosynthesis:

$$270 \quad ^{13}\epsilon_p = \epsilon_{\text{diff}} + (C_{\text{up}} / (C_{\text{up}} + 1/\text{var})) \cdot \delta_{\text{d}^{13}\text{C}} + \theta \cdot (\epsilon_{\text{fix}} - \epsilon_{\text{diff}}) \quad (24)$$

where

$$\theta = (1 + (C_{\text{up}} - 1) \cdot \text{var}) / (1 + C_{\text{up}} \cdot \text{var}) \quad (25)$$

and

$$\text{var} = \mu / \text{CO}_2^* \cdot 1000 \cdot Q_c / (\text{cell}_{\text{permea}} \cdot \text{cell}_{\text{surf}}) \quad (26)$$

275 with Q_c being the cell carbon content, $\text{cell}_{\text{permea}}$ being the cell wall permeability to CO_2 (aq), $\text{cell}_{\text{surf}}$ being the surface areas of cells, C_{up} being the ratio of active carbon uptake to carbon fixation, ϵ_{fix} being a constant phytoplankton-type dependent fractionation effect of carbon fixation, $\epsilon_{\text{diff}} = 0.7$ representing the fractionation by diffusion (O'Leary, 1984), and $\delta_{\text{d13C}} = -9.0$ being the difference between the isotopic compositions of the external CO_2 and the organic matter pools (Goericke et al.,
280 1994).

While the fractionation during calcium carbonate formation is much smaller than the fractionation during photosynthesis (Turner, 1982), we include a small constant fractionation of 2‰ for calcium carbonate formation, based on work by Ziveri et al. (2003) –that found a range of 3‰ to –2‰ for different species. Other implementations of ^{13}C in ocean models have used values of 1‰ (e.g. Sonnerup et al., 1999; Tagliabue and Bopp, 2008) or have assumed no isotopic fractionation for calcification (e.g. Marchal et al., 1998; Schmittner et al., 2013) . However, as shown by Schmittner et al. (2013) , the effect of the calcium carbonate pump on $\delta^{13}\text{C}$ is small, so the choice of the value for the fractionation during calcium carbonate formation is not expected to have a big impact on the results in the current ecosystem model with one species of calcium carbonate.
285

290 3.2.4 Biotic ^{14}C

The ^{14}C air sea flux is calculated in the same way as shown in Eq. (15) for ^{13}C , but with the fractionation for ^{14}C being twice as large as for ^{13}C ($\epsilon_{14} = 2 \cdot \epsilon_{13}$, Zeebe and Wolf-Gladrow, 2001) and with $R^{14}\text{C}_{\text{atm}}$ and $R^{14}\text{C}_{\text{DIC}}$ instead of $R^{13}\text{C}_{\text{atm}}$ and $R^{13}\text{C}_{\text{DIC}}$. The biological fractionation is also the same as for ^{13}C , except that $\epsilon_{14} = 2 \cdot \epsilon_{13}$ everywhere in Sect. 3.2.3. The surface reference value
295 for DI^{14}C for the virtual flux calculation is $1944 \mu\text{mol m}^{-3}$, the same as for DI^{13}C (and DI^{12}C).

In contrast to ^{13}C , ^{14}C decays in all carbon pools, following the decay equation (see Eq. (11) in Sect. 3.1.2).

To compare the model simulated $\delta^{14}\text{C}$ values that we save as diagnostics (see Eq. 14) with published observations of $\Delta^{14}\text{C}$, we apply the same fractionation correction to it that is used for obser-
300 vations to convert $\delta^{14}\text{C}$ to $\Delta^{14}\text{C}$:

$$\Delta^{14}\text{C} = \delta^{14}\text{C} - 2(\delta^{13}\text{C} + 25)(1 + \delta^{14}\text{C}/1000). \quad (27)$$

In the following we always show $\Delta^{14}\text{C}$.

As for the abiotic ^{14}C implementation, the value of $\Delta^{14}\text{C}_{\text{atm}}$ can be set to be a constant or it can be read in from three files (one for the Northern Hemisphere, one for the equatorial region, and one
305 for the Southern Hemisphere).

3.3 Ecosystem driver

We added an ecosystem driver (`ecosys_driver`) to the ocean model of the CESM in order to make it easier to expand the model to carry additional passive tracers that require variables from the ecosystem model, without adding these additional tracers to the ecosystem model itself. The
310 ecosystem driver is structured similar to the `passive_tracers` subroutine that calls all passive tracer modules, but it handles only the passive tracers that use the ecosystem model (see Fig. 1). It is called from the `passive_tracers` subroutine, and determines how many ecosystem-related passive tracers the model carries based on the namelist options set at buildtime. It then calls all subroutines in the ecosystem model and the related tracer modules, after being called by passive
315 tracers with the corresponding tracer indices. Variables computed in the ecosystem model but used by other modules are shared via the new `ecosys_share` module. Only the ecosystem model changes the value of the variables in `ecosys_share` at this point. Other modules currently only read them from there, but do not modify them. With this infrastructure in place, additional tracers can be easily added without changing the ecosystem model too much. The only changes to the
320 ecosystem model should be the copying of ecosystem variables to `ecosys_share` if they need to be shared with a new module as well as potentially the addition of new definitions and calculations of derived ecosystem variables that are needed but that are not currently computed in the ecosystem model (or not present in the required format, i.e., defined as local 2-D variables instead of a global 3-D variable). Nitrogen isotopes in the ocean model have already been added using this infrastructure
325 (S. Yang, personal communication, 2014).

4 Results

4.1 Simulations and spin-up

We have performed several simulations with the new carbon-isotope enabled model. As described in Sect. 2, we used the ocean-only version of the CESM1.0.5, at a nominal 3° horizontal resolution,
330 forced by CORE-II climatological forcing (Large and Yeager, 2009). To spin up the carbon isotopes, we performed spin-up simulations that lasted several thousands of years. Radiocarbon takes a long time (5000–15 000 years, according to Orr et al., 2000) to equilibrate, due to the long timescale of deep ocean ventilation.

The abiotic radiocarbon has been spun-up for 10 000 years using an atmospheric CO_2 concentration of 284.7 ppm and a $\Delta^{14}\text{C}$ value of 0‰. The abiotic DI^{14}C and DI^{12}C were started from the
335 standard ecosystem initial conditions, scaled to yield a global initial state of 0‰ $\Delta^{14}\text{C}$ (following

Orr et al., 2000), in order to simplify early interpretation and code verification. After 10 000 simulated years, the models satisfies the OCMIP2 surface CO₂ flux criteria of less than 0.01 Pg C year⁻¹. In terms of the drift in Δ¹⁴C, 91 % of the ocean volume is spun-up to the OCMIP2 criteria of a drift of less than 0.001 ‰ year⁻¹ (compared to the required 98 % for OCMIP2). Compared to the fully-spun-up solution (obtained using a new online Newton–Krylov method, manuscript in preparation by K. Lindsay, NCAR), differences are seen in the deep ocean only.

For the biotic carbon isotopes, we spun-up the carbon isotopes for ~~3560–6010~~ years, starting from the initial conditions of the ecosystem model, scaled to give a δ¹³C of 0 ‰ and a Δ¹⁴C of –100 ‰. The atmospheric CO₂ concentration was set to 284.7 ppm, the atmospheric Δ¹⁴C was set to 0 ‰, and the atmospheric δ¹³C was set to –6.379 ‰. In order to study the different biological fractionation parameterizations, two additional ~~1000-year-long~~ spin-up simulations were branched from the first spin-up simulation at year 2560 and run to year ~~3560~~. ~~After 3560–6010~~. After 6010 years, the surface CO₂ flux is well below the OCMIP2 criteria of less than 0.01 Pg C year⁻¹, and over 99.99 % of the ocean volume show a drift of less than 0.001 ‰ year⁻¹ in δ¹³C. However, only ~~526~~ % of the ocean satisfies the OCMIP2 criteria of a drift of less than 0.001 ‰ year⁻¹ for Δ¹⁴C. ~~If Another 4000 years or more are likely required to get the biotic Δ¹⁴C fully spun-up according to the OCMIP2 criteria. However, if~~ we weaken the OCMIP2 criteria by an order of magnitude to less than 0.01 ‰ year⁻¹, ~~7599.98~~ % of the ocean satisfy this new criteria for Δ¹⁴C. ~~Hence, when comparing the biotic and abiotic in the following, we need to consider that we are comparing an almost spun-up state in the abiotic to a still drifting state in the biotic.~~ Due to the long time required to run the ocean model with the ecosystem and the biotic carbon isotopes (the ~~3560–6010~~ years took over ~~4–7~~ months of constant running on a supercomputer), we are currently not able to run the biotic radiocarbon to full equilibrium. In order to reach equilibrium in the future, a fast spin-up technique for the ecosystem model is currently in development by Keith Lindsay and will be applied to the biotic carbon isotopes when it is ready. We believe that for the purpose of this paper, which mainly documents the implementation of the carbon isotopes in the model, the current spin-up is sufficient. For other science applications, however, the biotic radiocarbon ~~would~~ will need to be spun up further in order to be fully trustworthy.

We then performed experiments from 1765 to 2008, with the initial conditions from the end of the spin-up simulations in year ~~3560–6010~~ for the biotic carbon isotopes and in year 10 000 for the abiotic radiocarbon. The atmospheric CO₂, Δ¹⁴C, and δ¹³C was prescribed based on the OCMIP-2 files (Orr et al., 2000) up to 1989, and H. Graven’s formulation of the global average for 1990–2008 (personal communication, 2012). The atmospheric state was the same repeating climatological CORE-II forcing as used for the spin-up, so changes related to warming or changes in the wind forcing over the 20th century are not included. ~~At the same time, we~~ We continued with the climatological CORE-II forcing rather than use the interannually varying CORE-II forcing for 1948–2007 in order to avoid shocks to the ocean when switching the forcing and when the forcing jumps from 2007

back to 1948 every 60 years. This jump in the forcing impacts the simulation for 10 years or more
375 (as described in Danabasoglu et. al., 2014), and would overlap with the start of the introduction of
bomb radiocarbon into the atmosphere.

We also continued the spin-up simulations for 243 years, so that we could remove the influence
of a any continuing drift on the radiocarbon results shown in Sect. 4.2.2. To investigate the influence
of the net CO₂ uptake on the simulation results in the second part of the 20th century, we also
380 performed sensitivity experiments where the atmospheric CO₂ was fixed at 1949 conditions, while
 $\Delta^{14}\text{C}_{\text{atm}}$ and $\delta^{13}\text{C}_{\text{atm}}$ changed as usual.

4.2 ¹⁴C results

4.2.1 Simulated distributions of $\Delta^{14}\text{C}$

The radiocarbon simulation shows good agreement with the gridded GLODAP data for the 1990s
385 (Key et al., 2004), reflecting the main features of the $\Delta^{14}\text{C}$ distribution: (i) at the surface (see Fig. 2)
the model shows the observed M-shape of $\Delta^{14}\text{C}$ distribution, with the highest values in the relatively
stable subtropical waters, intermediate values in the equatorial upwelling zone, and low values in the
polar regions, where the residence time is short and sea ice limits the uptake of atmospheric $\Delta^{14}\text{C}$,
with the overall lowest values in the Southern Ocean, where the upwelling of old, low $\Delta^{14}\text{C}$ waters
390 further dilutes the surface waters. (ii) In the zonal mean (see Fig. 3), newly formed deepwater with
high $\Delta^{14}\text{C}$ values can clearly be separated from old water masses with low $\Delta^{14}\text{C}$ values. (iii) In the
depth profiles (see Fig. 4), it is obvious that the $\Delta^{14}\text{C}$ in the deep water decreases from the Atlantic
Ocean over the Indian Ocean to the Pacific Ocean, which has the lowest $\Delta^{14}\text{C}$ values (i.e., oldest
water). Consistently, the abiotic $\Delta^{14}\text{C}$ values are higher than the biotic $\Delta^{14}\text{C}$ values, but both
395 show the same general features also shown in GLODAP (Key et al., 2004) and in the cruise data
compiled by Schmittner et al. (2013) because their distribution is set mainly by the physical ocean
simulation. The ~~differences~~ difference between the abiotic and biotic simulation due to biological
effects ~~is difficult to determine at this point, as the biotic simulation is much~~ has been estimated to
~~be on the order of 10% (Fiadiero, 1982), but since the biotic radiocarbon simulation is~~ less spun-up
400 than the abiotic simulation. ~~This at this point, a detailed investigating of the impact of the biological
effects is premature and~~ will be the topic of a future study when we can spin-up both radiocarbon
implementations using a fast-spin up technique.

Above 1000 m, the depth structure of the simulated $\Delta^{14}\text{C}$ agrees reasonably well with observa-
tions, with the best agreement with the GLODAP $\Delta^{14}\text{C}$ in the upper 250 m of the Indian Ocean
405 (see Fig. 4). The largest biases are found at depth below 1000 m (see Fig. 4), with the model show-
ing $\Delta^{14}\text{C}$ values that are too negative (i.e., water that is too old). The largest bias is located in
the deep Pacific, where the $\Delta^{14}\text{C}$ is up to 100‰ too negative (see Figs. 3 and 4). In terms of
radiocarbon age, the maximum bias in the deep Pacific is 1000 years compared to GLODAP, re-

vealing that the deep Pacific Ocean in the model is not ventilated as much as it should be. This
410 ~~bias is a well known bias in the CESM, which~~ was also present in the ocean model of a previous
version of the CESM, the CCSM3 (Graven et al., 2012), as well as in the nominal 1° resolution ver-
sion of the current CESM1 ocean model (Bardin et al., 2014), ~~and is related to too weak Antarctic~~
~~Bottom Water formation in the CESM (Danabasoglu et. al., 2011) and too shallow mixed layers in~~
~~the Southern Ocean (Moore et al., 2013)~~. Currently radiocarbon is being used to test improvements
415 to the ~~ventilation in the Southern Ocean in the~~ ocean model in the CESM, in order to improve this
bias in future versions of the CESM (K. Lindsay, personal communication, 2014).

4.2.2 ^{14}C bomb inventory

The excess oceanic radiocarbon inventory is frequently ~~being~~-used to investigate the ocean uptake of
anthropogenic carbon (e.g. Key et al., 2004; Graven et al., 2012) and to determine the mean gas ex-
420 change velocity used in ocean models (e.g. Wanninkhof, 1992; Sweeney et al., 2007; Naegler et al.,
2006; Naegler, 2009). To establish how well the newly developed radiocarbon tracer compares to
observations, we here compare the simulated excess radiocarbon inventory with observational esti-
mates. The excess radiocarbon in the ocean includes change in the oceanic radiocarbon from the
atmospheric nuclear bomb tests of the 1950s and 1960s, as well as from the Suess effect and changes
425 in net CO_2 uptake, compared to the reference period of the 1940s, following Naegler (2009). In
1975, the excess radiocarbon inventory in the abiotic and biotic simulation is ~~286×10^{26}~~ ~~297×10^{26}~~
atoms ^{14}C and ~~291×10^{26}~~ ~~295×10^{26}~~ atoms ^{14}C , respectively. This lies within the range of obser-
vational estimates of the excess radiocarbon in 1975, which range from 225×10^{26} atoms ^{14}C to
 $314 \pm 35 \times 10^{26}$ atoms ^{14}C (see Table 2). It has been shown that the earlier estimates from Broecker
430 et al. (1985, 1995) were high by about 25 % (e.g. Hesshaimer et al., 1994; Peacock, 2004; Sweeney
et al., 2007), which suggests that the simulated values are probably on the high end of the observa-
tional range. One reason for this could be the choice of the coefficient $a = 0.31 \text{ cm h}^{-1}$ in Eq. (3),
which has been shown to be high (e.g. Sweeney et al., 2007; Naegler, 2009). Graven et al. (2012)
showed that in the ocean model of the CCSM3, the simulated excess radiocarbon inventory was
435 lower when a coefficient $a = 0.23 \text{ cm h}^{-1}$ rather than $a = 0.31 \text{ cm h}^{-1}$ was used in Eq. (3). How-
ever, since $a = 0.31 \text{ cm h}^{-1}$ is the parameter used in the CESM in general to compute air-sea gas
fluxes, we did not change it here. For 1995, the excess radiocarbon ~~inventory inventories~~ in the abi-
otic and biotic simulation are ~~372×10^{26}~~ ~~389×10^{26}~~ atoms ^{14}C and ~~384×10^{26}~~ ~~390×10^{26}~~ atoms
 ^{14}C , respectively, which ~~agrees well with~~ ~~is close to but slightly higher than~~ the observational esti-
440 mates of $313\text{--}383 \times 10^{26}$ atoms ^{14}C ~~, particularly the most recent estimate from Naegler (2009) and~~
~~the corrected estimates from Key et al. (2004)~~ (see Table 2).

The natural radiocarbon inventory, before anthropogenic disturbances from the Suess effect and
from increased oceanic net CO_2 uptake, has been estimated to be $19000 \pm 1200 \times 10^{26}$ atoms of ^{14}C
(Naegler, 2009). In the ~~model simulation~~ the inventory is ~~within just outside~~ the error bar for the

445 biotic model ($17\ 959\text{--}17\ 964 \times 10^{26}$ – $763\text{--}17\ 770 \times 10^{26}$ atoms of ^{14}C , depending on the biological
fractionation used), and slightly lower for the abiotic model ($16\ 730 \times 10^{26}$ – $16\ 190 \times 10^{26}$ atoms of
 ^{14}C). ~~These~~ The natural radiocarbon inventories are calculated for years ~~3735–3744~~ 6185–6194
of the control simulations, which corresponds to the same total runtime as years 1940–1949 in the
1765–2008 experiments, which were started from the control in year ~~3560~~–~~To~~ 6010. ~~However,~~
450 the biotic model estimate of the natural radiocarbon inventory might still not be the final value, as
the biotic radiocarbon is still spinning-up. In terms of the anthropogenic radiocarbon inventories
presented next, this biases should not play any large role, however, as we remove any remaining
drift. Specifically, to calculate the early anthropogenic radiocarbon inventory present in the 1940s,
we take the difference between the natural radiocarbon inventory in simulation years ~~3735–3744~~
455 6185–6194 (with constant atmospheric CO_2 , $\Delta^{14}\text{C}$, and $\delta^{14}\text{C}$) and the inventory in the 1940s (with
changing atmospheric CO_2 , $\Delta^{14}\text{C}$, and $\delta^{14}\text{C}$ since 1765). By taking this difference between years of
equal total runtime, we remove the impact of any remaining drift in $\Delta^{14}\text{C}$. We find an anthropogenic
radiocarbon inventory of 20×10^{26} atoms of ^{14}C for the abiotic model and 5×10^{26} atoms of ^{14}C
for the biotic model (independent of the biological fractionation used). Both of these anthropogenic
460 radiocarbon inventories for the 1940s are within the error bar of the estimate of $4 \pm 20 \times 10^{26}$ of ^{14}C
from Naegler (2009), with the biotic model giving a very good match.

Using sensitivity experiments from 1950–2008 with atmospheric CO_2 held constant at 1949 levels
but normally increasing atmospheric $\Delta^{14}\text{C}$, we can calculate the impact of increased ocean uptake
of anthropogenic CO_2 on the excess radiocarbon inventory: in 1975, the excess oceanic radiocar-
465 bon inventory relative to the 1940s due to ~~atmospheric~~–~~atmospheric~~ $\Delta^{14}\text{C}$ changes alone (from the
atmospheric bomb tests and the Suess effect) is ~~271×10^{26} – 282×10^{26}~~ atoms of ^{14}C for the abiotic
model and ~~276×10^{26} – 280×10^{26}~~ atoms of ^{14}C for the biotic model, while for 1995 the numbers are
 ~~336×10^{26} – 353×10^{26}~~ atoms of ^{14}C and ~~348×10^{26} – 354×10^{26}~~ atoms of ^{14}C , respectively. This
means that the increase in net CO_2 uptake contributed 15×10^{26} atoms of ^{14}C in 1975 and 36×10^{26}
470 atoms of ^{14}C in 1995 compared to the 1940s (for both the abiotic and biotic models), which is 5
and 9 % of the total radiocarbon excess in these years. These changes are in excellent agreement
with calculations from Naegler (2009), which showed an excess radiocarbon inventory in 1995 of
 $346 \pm 98 \times 10^{26}$ atoms ^{14}C due to atmospheric $\Delta^{14}\text{C}$ changes, and $27 \pm 9 \times 10^{26}$ atoms ^{14}C due to
net CO_2 uptake. The percentage contribution of the net CO_2 uptake to the total radiocarbon excess
475 was given as 3 % in 1975 and 8 % in 1995 in Naegler (2009), which again compares very well with
our model simulation.

4.3 ^{13}C results

4.3.1 Simulated $\delta^{13}\text{C}$ and the impact of different biological fractionation parameterizations

480 In the literature, models of biological fractionation are still under debate (e.g. Keller and Morel, 1999). We therefore tested three different parameterizations of biological fractionation, to investigate the impact on the simulated $\delta^{13}\text{C}$ (as described in Sects. 3.2.3 and 4.1). As shown in Fig. 5a, the simulated globally averaged ϵ_p depth profiles differ when these different parameterizations are used, with ϵ_p values ranging from 15–30. By design, ϵ_p is the same for diatoms, diazotrophs, and small
485 phytoplankton when using Rau et al. (1989), while ϵ_p shows large variations between species for the method of Keller and Morel (1999), due to the dependence on species-specific cell parameters (see Table 1). The method of Laws et al. (1995) leads to small differences between species in the surface ocean only. Below 200 m, only the ϵ_p following Rau et al. (1989) still changes with depth (see Fig. 5a), due to the sole dependence of ϵ_p on CO_2^* and the export of organic carbon and carbonates
490 to depth.

The impact of the different biological fractionation choices on $\delta^{13}\text{C}_{\text{DIC}}$ is noticeable (see Fig. 5b), with the globally-averaged $\delta^{13}\text{C}_{\text{DIC}}$ based on ϵ_p from Rau et al. (1989) being larger below 150 m compared to the $\delta^{13}\text{C}_{\text{DIC}}$ from Laws et al. (1995) and Keller and Morel (1999), but slightly smaller at the surface. Despite the more complex formulation of ϵ_p in Keller and Morel (1999) compared to
495 Laws et al. (1995) and the significantly different ϵ_p profiles, the resulting $\delta^{13}\text{C}_{\text{DIC}}$ from both methods is very similar and only differs slightly at depth (most notably between 150 and 2000 m). To compare the simulated $\delta^{13}\text{C}_{\text{DIC}}$ to the cruise data of $\delta^{13}\text{C}_{\text{DIC}}$ compiled by Schmittner et al. (2013), we re-gridded the model output to subsample the model at the same points as covered by the cruise data. The resulting globally-averaged depth profiles are shown in Fig. 5c, and are remarkably similar to the
500 full globally-averaged model results in Fig. 5b. Both show the expected increase in $\delta^{13}\text{C}_{\text{DIC}}$ directly below the surface, due to the preferential uptake of the light isotope during photosynthesis, followed by the expected decrease of $\delta^{13}\text{C}_{\text{DIC}}$ with depth due to the remineralization of the isotopically light organic material back into the water column. The model simulated global depth-profile of $\delta^{13}\text{C}_{\text{DIC}}$ lies within the error range of $\pm 0.2\text{‰}$ around the cruise $\delta^{13}\text{C}_{\text{DIC}}$ data between the surface and 150 m
505 and below 1000 m, but shows smaller $\delta^{13}\text{C}_{\text{DIC}}$ values than observed between 150 and 1000 m.

For individual basins, the model bias compared to the cruise data is smallest in the Atlantic, with the $\delta^{13}\text{C}_{\text{DIC}}$ based on the biological fractionation from Rau et al. (1989) almost entirely within the uncertainty range of the data (see Fig. 5d). All three basins contribute to the bias seen between 150 and 2000 m in the global average, with the Indian Ocean contributing the most to this bias in the
510 upper ocean and the Pacific Ocean contributing the most at intermediate depths (see Fig. 5c–f). In general, the model simulated $\delta^{13}\text{C}_{\text{DIC}}$ tends to be smaller than the observed $\delta^{13}\text{C}_{\text{DIC}}$. While the difference between the full global average in the model and the subset global average based on the

cruise data locations is small, the difference between the total basin average (shown as dashed lines in Fig. 5d–f) and the subset basin averages (shown as solid lines) is larger for the individual basins.

515 At the surface, the simulated $\delta^{13}\text{C}_{\text{DIC}}$ values show a systematic bias in that they are generally larger than the observational data suggests, but the same general spatial pattern is visible (see Fig. 6). While both gas-exchange and biological process are important for the surface ocean $\delta^{13}\text{C}_{\text{DIC}}$ pattern (Schmittner et al., 2013), the details of the biological fractionation parameterizations appear to have a very small impact at the surface, as shown in the almost identical surface distributions from the
520 model (see Fig. 6c–e). The zonal means of $\delta^{13}\text{C}_{\text{DIC}}$ from the different biological fractionation parameterizations on the other hand do show some small differences (see Fig. 7), with the biological fractionation from Rau et al. (1989) leading to the largest $\delta^{13}\text{C}_{\text{DIC}}$ values in all three ocean basins, while the fractionation based on Keller and Morel (1999) shows the lowest $\delta^{13}\text{C}_{\text{DIC}}$ values. Overall all three parameterizations lead to the expected pattern of high values of $\delta^{13}\text{C}_{\text{DIC}}$ in water that has
525 recently been in contact with the surface (e.g., North Atlantic Deep Water) and low $\delta^{13}\text{C}_{\text{DIC}}$ values in water that has been out-of-contact with the atmosphere for a long period of time and has accumulated a large amount of remineralized (isotopically light) organic matter (e.g., in the deep Pacific).

We choose the biological formulation from Laws et al. (1995) as the default biological fractionation in our model, as it considers the growth rate of different species, but the differences in the
530 simulated $\delta^{13}\text{C}_{\text{DIC}}$ compared to the more complex formulation from Keller and Morel (1999) is small. The other parameterizations of biological fractionation remain an option in the model that can be chosen at build time.

4.3.2 Oceanic surface ^{13}C Suess effect

The surface oceanic Suess effect, which is the decrease in the surface ocean $\delta^{13}\text{C}$ due to the penetration of carbon originating from the burning of fossil fuels, has been calculated from observational
535 data as well as from other models that include ^{13}C , and it is often used to derive the oceanic anthropogenic carbon uptake (e.g. McNeil et al., 2001; Tagliabue and Bopp, 2008). In our model simulation, the surface $\delta^{13}\text{C}$ change between 1975 and 1995 is -0.159 – -0.164 to -0.163 – -0.167 ‰ decade $^{-1}$ (the range is for the different biological fractionations used). This compares well with other estimates of -0.171 ‰ decade $^{-1}$ (Bacastow et al., 1996), -0.018 – -0.18 ‰ decade $^{-1}$ (Gruber et al.,
540 1999), -0.15 ‰ decade $^{-1}$ (Sonnerup et al., 1999), and -0.174 ‰ decade $^{-1}$ (Tagliabue and Bopp, 2008). As already shown by Quay et al. (1992) and Gruber et al. (1999), the surface ocean Suess effect is not uniform (see Fig. 8), and the model simulation of the spatial Suess effect agrees well with the model results of Tagliabue and Bopp (2008): the largest changes (i.e., most negative values
545 in Fig. 8) occur in regions with little deep ventilation and therefore longer residence times of water at the surface (e.g., the subtropical gyres) while the smallest changes (i.e., least negative or zero in Fig. 8) occur in regions of reduced air–sea gas exchange (e.g., under sea ice), in regions with active deep convection (and therefore short residence times at the surface, e.g. around Antarctic), as well

as in regions with upwelling (which dilutes the surface $\delta^{13}\text{C}$, for example off the west coast of South
550 America).

Compared to the pre-industrial ocean, the total surface ocean ^{13}C Suess effect is -0.064 to
 -0.066 0.065 ‰ decade $^{-1}$ for 1860–2000 (depending on the different fractionationsbiological fractionation
used), compared to -0.07 ‰ decade $^{-1}$ found by Tagliabue and Bopp (2008). The fact that the sim-
555 ulated oceanic ^{13}C Suess effect calculated over different periods agrees reasonably well with other
available estimates suggests that our model is able to simulate the change in the oceanic $\delta^{13}\text{C}$ in-
ventory correctly, despite some mean biases in the distribution of $\delta^{13}\text{C}$ described and shown in
Sect. 4.3.1.

5 Changes in CESM1.2

In CESM1.2, the ocean ecosystem model prescribes the input of nutrients and carbon by rivers,
560 while in CESM1.0 rivers only added a virtual salt flux to the ocean. This means that for the biotic
carbon isotope implementation in CESM1.2, we also need to add an isotopic carbon flux. Based on
published research, we assume that globally, the $\delta^{13}\text{C} = -10$ ‰ for DI (Mook, 1986; Raymond et al., 2004) and
the $\delta^{13}\text{C} = -27.6$ ‰ for DO (Raymond et al., 2004). The river runoff values of for and DO use the
following constant global values to multiply the normal carbon fluxes from rivers in the ecosystem
565 model: $\Delta^{14}\text{C} = -50$ ‰ for DO and $\Delta^{14}\text{C} = \Delta^{14}\text{C}_{\text{atm}} - 50$ ‰ (e.g. Mook, 1986; Raymond et al., 2004).

The other notable change in the ecosystem model in CESM1.2 compared to the CESM1.0 that
affects the carbon isotopes is the addition of bottom sediment cells. In CESM1.0 everything in the
bottom cell was remineralized, while in CESM1.2 sedimentary burial and denitrification losses are
calculated based on empirical relations (Dunne et al., 2007; Bohlen et al., 2012; Soetaert et al., 1996) and
570 calcite is preserved in sediments above the lysocline (defined at a constant depth of 3300), and
dissolves below. The biotic carbon isotope code was adapted to also account for these processes.

5 Summary

We have developed carbon isotope tracers in the ocean model of the CESM, including a biotic and an
abiotic radiocarbon tracer and a biotic ^{13}C tracer. The details of the implementation are described
575 here in order to serve as reference for future users of these new model features and/or for model
developers planning to modify the code or add carbon isotopes to other ocean models. In particular,
we tested three different formulations for the fractionation during phytoplankton growth that have
been discussed in the literature, and show that the effect on the simulated $\delta^{13}\text{C}$ in the ocean is
relatively minor. A comparison of the simulation results from the coarse nominal-3° resolution ocean
580 model with forced with climatological CORE-II atmospheric forcing and with present-day data for
 $\Delta^{14}\text{C}$ and $\delta^{13}\text{C}$ shows that the simulated carbon isotopes can represent the large-scale features of
the observed distributions as well as the anthropogenic changes due to nuclear bomb tests and the

burning of fossil fuels. The carbon isotopes also ~~reveal some~~ reflect some known model biases, for example a too sluggish ventilation of the deep Pacific Ocean. Once a fast-spin up technique
585 for the biotic carbon isotopes has been implemented, we are planning to further validate the ~~model~~
carbon-isotope simulation in the fully-coupled CESM framework at 1° resolution. Ultimately, we plan to use the carbon isotopes for both present-day and paleo simulations in the fully-coupled framework of the CESM at the standard nominal 1° resolution in the ocean, in order to investigate details of changes in the ocean circulation over the 20th century, the last Millennium, and at the Last
590 Glacial Maximum.

Code availability

~~The carbon isotope code and the~~ The newly developed carbon isotope and ecosystem driver code for the CESM1.0.5 is included as supplementary material here. The carbon isotope code has been updated to the CESM1.2, and has been added to the ocean development trunk in the CESM SVN
595 repository (as of version cesm1-3-beta10). It continues to be updated as the CESM evolves, and is targeted for public release as part of the ~~CESM1.3 in 2015.~~ CESM2 in 2016. At that point the code will be available through the ~~CESM1.3~~ CESM release website at <https://www2.cesm.ucar.edu/models/current>. Prior to the release, developer access can already be applied for at <https://www2.cgd.ucar.edu/sections/cseg/development-code>, subject to the CESM development guidelines.

600 *Acknowledgements.* A. Jahn was funded under the DOE SciDAC grant “Development of an Isotope-Enabled CESM for Testing Abrupt Climate Changes” (DE-SC0006744). We thank Michael Levy (NCAR) and David M. Hall (CU Boulder) for software engineering advice, Matt Long (NCAR) for helpful discussions, and Heather Graven (Scripps) for sharing her extensions of the OCMIP atmospheric $\Delta^{14}\text{C}$, $\delta^{13}\text{C}$, and CO_2 data with us. We also thank Guy Munhoven for serving as editor and two anonymous reviewers for their constructive comments
605 on the discussion paper. NCAR is sponsored by the National Science Foundation. N. Gruber and X. Giraud acknowledge funding from ETH Zürich. Computing resources (ark:/85065/d7wd3xhc) were provided by the Climate Simulation Laboratory at NCAR’s Computational and Information Systems Laboratory on Yellowstone (2012), sponsored by the National Science Foundation and other agencies. Data analysis was performed with NCL Version 6.2.0 (2014).

610 References

- Bacastow, R. B., Keeling, C. D., Lueker, T. J., Wahlen, M., and Mook, W. G.: The ^{13}C Suess Effect in the world surface oceans and its implications for oceanic uptake of CO_2 : analysis of observations at Bermuda, *Global Biogeochem. Cy.*, 10, 335–346, [doi:10.1029/96GB00192](https://doi.org/10.1029/96GB00192), 1996.
- Bardin, A., Primeau, F., and Lindsay, K.: An offline implicit solver for simulating prebomb radiocarbon, *Ocean Modelling*, 73, 45–58, [doi:10.1016/j.ocemod.2013.09.008](https://doi.org/10.1016/j.ocemod.2013.09.008), 2014.
- 615 Bigeleisen, J.: The effects of isotopic substitutions on the rate of chemical reactions, *J. Phys. Chem.*, 56, 823–828, 1952.
- Bohlen, L., Dale, A., and Wallmann, K.: Simple transfer functions for calculating benthic fixed nitrogen losses and C:N:P regeneration ratios in global biogeochemical models, *Global Biogeochem. Cy.*, 26, GB3029, [doi:10.1029/2011GB004198](https://doi.org/10.1029/2011GB004198), 2012.
- 620 Broecker, W. S. and Peng, T.-H.: Stratospheric contribution to the global bomb radiocarbon inventory: model versus observation, *Global Biogeochem. Cy.*, 8, 377–384, [doi:10.1029/94GB00680](https://doi.org/10.1029/94GB00680), 1994.
- Broecker, W. S., Peng, T. H., and Engh, R.: Modelling the carbon system, *Radiocarbon*, 22, 377–384, 1980.
- Broecker, W. S., Peng, T.-H., Östlund, G., and Stuiver, M.: The distribution of bomb radiocarbon in the ocean, *J. Geophys. Res.*, 90, 6953–6970, [doi:10.1029/JC090iC04p06953](https://doi.org/10.1029/JC090iC04p06953), 1985.
- 625 Broecker, W. S., Sutherland, S., Smethie, W., Peng, T. H., and Östlund, G.: Oceanic radiocarbon: separation of the natural and bomb components, *Global Biogeochem. Cy.*, 9, 263–288, [doi:10.1029/95GB00208](https://doi.org/10.1029/95GB00208), 1995.
- Craig, H.: Carbon 13 in plants and the relationship between carbon 13 and carbon 14 variations in nature, *J. Geol.*, 62, 115–149, 1954.
- 630 Craig, H.: Isotopic standards for carbon and oxygen and correction factors for mass-spectrometric analysis of carbon dioxide, *Geochim. Cosmochim. Ac.*, 12, 133–149, 1957.
- Crucifix, M.: Distribution of carbon isotopes in the glacial ocean: a model study, *Paleoceanography*, 20, PA4020, [doi:10.1029/2005PA001131](https://doi.org/10.1029/2005PA001131), 2005.
- 635 Curry, W. B. and Oppo, D. W.: Glacial water mass geometry and the distribution of $\delta^{13}\text{C}$ of $p\text{CO}_2$ in the Western Atlantic Ocean, *Paleoceanography*, 20, PA1017, [doi:10.1029/2004PA001021](https://doi.org/10.1029/2004PA001021), 2005.
- [Danabasoglu, G., S. C. Bates, B. P. Briegleb, S. R. Jayne, M. Jochum, W. G. Large, S. Peacock, and S. G. Yeager: The CCSM4 Ocean Component, J. Climate, 25, 1361–1389, doi:http://dx.doi.org/10.1175/JCLI-D-11-00091.1, 2012.](https://doi.org/10.1175/JCLI-D-11-00091.1)
- 640 [Danabasoglu, G., S. G. Yeager, D. Bailey, E. Behrens, M. Bentsen, D. Bi, A. Biastoch, C. Böning, A. Bozec, V. M. Canuto, C. Cassou, E. Chassignet, A. C. Coward, S. Danilov, N. Diansky, H. Drange, R. Farneti, E. Fernandez, P. G. Fogli, G. Forget, Y. Fujii, S. M. Griffies, A. Gusev, P. Heimbach, A. Howard, T. Jung, M. Kelley, W. G. Large, A. Leboissetier, J. Lu, G. Madec, S. J. Marsland, S. Masina, A. Navarra, A. J. George Nurser, A. Pirani, D. Salas y Melia, B. L. Samuels, M. Scheinert, D. Sidorenko, A.-M. Treguier, H. Tsujino, P. Uotila, S. Valcke, A. Voldoire, Q. Wang: North Atlantic simulations in Coordinated Ocean-ice Reference Experiments phase {II} \(CORE-II\). Part I: Mean states, Ocean Modelling, 73, 76–107, doi:http://dx.doi.org/10.1016/j.ocemod.2013.10.005, 2014.](https://doi.org/10.1016/j.ocemod.2013.10.005)
- 645 Doney, S. C., Lindsay, K., Caldeira, K., Campin, J., Drange, H., Dutay, J., Follows, M., Gao, Y., Gnanadesikan, A., Gruber, N., Ishida, A., Joos, F., Madec, G., Maier-Reimer, E., Marshall, J., Matear, R., Monfray, P.,

- 650 Mouchet, A., Najjar, R., Orr, J., Plattner, G., Sarmiento, J., Schlitzer, R., Slater, R., Totterdell, I., Weirig, M.,
Yamanaka, Y., and Yool, A.: Evaluating global ocean carbon models: the importance of realistic physics,
Global Biogeochem. Cy., 18, GB3017, [doi:doi:10.1029/2003GB002150](https://doi.org/10.1029/2003GB002150), 2004.
- Dunne, J. P., Sarmiento, J. L., and Gnanadesikan, A.: A synthesis of global particle export from the surface
ocean and cycling through the ocean interior and on the seafloor, Global Biogeochem. Cy., 21, GB4006,
655 [doi:doi:10.1029/2006GB002907](https://doi.org/10.1029/2006GB002907), 2007.
- Fiadiero, M. E.: Three-dimensional modeling of tracers in the deep Pacific Ocean: radiocarbon and the circu-
lation, J. Mar. Res., 40, 537–550, 1982.
- Galbraith, E. D., Kwon, E. Y., Gnanadesikan, A., Rodgers, K. B., Griffies, S. M., Bianchi, D., Sarmiento, J. L.,
Dunne, J. P., Simeon, J., Slater, R. D., Wittenberg, A. T., and Held, I. M.: Climate variability and radiocarbon
660 in the CM2Mc Earth System Model, J. Climate, 24, 4230–4254, [doi:doi:10.1175/2011JCLI3919.1](https://doi.org/10.1175/2011JCLI3919.1), 2011.
- Godwin, H.: Half life of radiocarbon, Nature, 195, 984, [doi:doi:10.1038/195984a0](https://doi.org/10.1038/195984a0), 1962.
- Goericke, R., Montoya, J. P., and Fry, B.: Physiology of isotopic fractionation in algae and cyanobacteria, in:
Stable Isotopes in Ecology and Environmental Science, edited by: Lajtha, K. and Michener, R. H., Blackwell
Scientific Publications, Oxford, 187–221, 1994.
- 665 Graven, H. D., Gruber, N., Key, R., Khatiwala, S., and Giraud, X.: Changing controls on oceanic radiocarbon:
new insights on shallow-to-deep ocean exchange and anthropogenic CO₂ uptake, J. Geophys. Res., 117,
C10005, [doi:doi:10.1029/2012JC008074](https://doi.org/10.1029/2012JC008074), 2012.
- Gruber, N. and Keeling, C. D.: The isotopic air–sea disequilibrium and the oceanic uptake of CO₂, in: Pro-
ceedings of the 2nd International Symposium CO₂ in the oceans, NIS, Tsukuba, Japan, edited by: Nojiri, Y.,
670 CGER-I037, Center for Global Environmental Research, National Institute for Environmental Studies, 245–
250, 1999.
- Gruber, N. and Keeling, C.: An improved estimate of the isotopic air–sea disequilibrium of CO₂: implications
for the oceanic uptake of anthropogenic CO₂, Geophys. Res. Lett., 28, 555–558, 2001.
- Gruber, N., Keeling, C. D., Bacastow, R. B., Guenther, P. R., Leuker, T. J., Wahlen, M., Meijer, H. A. J.,
675 Mook, W. G., and Stocker, T. F.: Spatiotemporal patterns of carbon-13 in the global surface oceans and the
oceanic Suess effect, Global Biogeochem. Cy., 13, 307–335, 1999.
- Hesse, T., Butzin, M., Bickert, T., and Lohmann, G.: A model-data comparison of $\delta^{13}\text{C}$ in the glacial Atlantic
Ocean, Paleoceanography, 26, PA3220, [doi:doi:10.1029/2010PA002085](https://doi.org/10.1029/2010PA002085), 2011.
- Hesshaimer, V., Heimann, M., and Levin, I.: Radiocarbon evidence for a smaller oceanic carbon dioxide sink
680 than previously believed, Nature, 370, 201–203, [doi:doi:10.1038/370201a0](https://doi.org/10.1038/370201a0), 1994.
- Hurrell, J., Holland, M. M., Ghan, P. R. G. S., Kushner, J. K. P., Lamarque, J.-F., Large, W. G., D. Lawrence, D.,
Lindsay, K., Lipscomb, W. H., Long, M., Mahowald, N., Marsh, D., Neale, R., Rasch, P., Vavrus, S.,
Vertenstein, M., Bader, D., Collins, W. D., Hack, J. J., Kiehl, J., and Marshall, S.: The Community
Earth System Model: a framework for collaborative research, B. Am. Meteorol. Soc., 94, 1339–1360,
685 [doi:doi:10.1175/BAMS-D-12-00121.1](https://doi.org/10.1175/BAMS-D-12-00121.1), 2013.
- Karlen, I., Olsson, I. U., Kallburg, P., and Kilici, S.: Absolute determination of the activity of two ¹⁴C dating
standards, Ark. Geofys., 4, 465–471, 1968.
- Keeling, C. D., Bacastow, R. B., and Tans, P. P.: Predicted shift in the ¹³C/¹²C ratio of atmospheric carbon
dioxide, Geophys. Res. Lett., 7, 505–508, [doi:doi:10.1029/GL007i007p00505](https://doi.org/10.1029/GL007i007p00505), 1980.

- 690 Keller, K. and Morel, F. M. M.: A model of carbon isotopic fractionation and active carbon uptake in phytoplankton, *Mar. Ecol.-Prog. Ser.*, 182, 295–298, 1999.
- Key, R. M., Kozyr, A., Sabine, C. L., Lee, K., Wanninkhof, R., Bullister, J. L., Feely, R. A., Millero, F. J., Mordy, C., and Peng, T.-H.: A global ocean carbon climatology: results from Global Data Analysis Project (GLODAP), *Global Biogeochem. Cy.*, 18, GB4031, [doi:doi:10.1029/2004GB002247](https://doi.org/10.1029/2004GB002247), 2004.
- 695 Large, W. G. and Yeager, S. G.: The global climatology of an interannually varying air–sea flux data set, *Clim. Dynam.*, 33, 341–364, [doi:doi:10.1007/s00382-008-0441-3](https://doi.org/10.1007/s00382-008-0441-3), 2009.
- Lassey, K. R., Manning, M. R., and O’Brien, B. J.: An overview of oceanic radiocarbon: its inventory and dynamics, *CRC Rev. Aquatic Sci.*, 3, 117–146, 1990.
- Laws, E. A., Bidigare, R. R., and Popp, B. N.: Effect of growth rate and CO₂ concentration on carbon isotopic fractionation by the marine diatom *Phaeodactylum tricornutum*, *Limnol. Oceanogr.*, 42, 1552–1560, 1997.
- 700 Laws, E. A., Popp, B. N., Bidigare, R. R., Kennicutt, M. C., and Macko, S. A.: Dependence of phytoplankton carbon isotopic composition on growth rate and [CO₂]_{aq}: theoretical considerations and experimental results, *Geochim. Cosmochim. Ac.*, 59, 1131–1138, [doi:doi:10.1016/0016-7037\(95\)00030-4](https://doi.org/10.1016/0016-7037(95)00030-4), 1995.
- Libby, W. F.: *Radiocarbon Dating*, 2nd edn., Univ. Chicago Press, 1955.
- 705 Marchal, O., Stocker, T. F., and Joos, F.: A latitude-depth, circulation-biogeochemical ocean model for paleoclimate studies. Development and sensitivities, *Tellus B*, 50, 290–316, [doi:doi:10.1034/j.1600-0889.1998.t01-2-00006.x](https://doi.org/10.1034/j.1600-0889.1998.t01-2-00006.x), 1998.
- Matsumoto, K., Sarmiento, J. L., Key, R. M., Aumont, O., Bullister, J. L., Caldeira, K., Campin, J., Doney, S. C., Drange, H., Dutay, J.-C., Follows, M., Gao, Y., Gnanadesikan, A., Gruber, N., Ishida, A.,
- 710 Joos, F., Lindsay, K., Maier-Reimer, E., Marshall, J., Matear, R., Monfray, P., Mouchet, A., Najjar, R., Plattner, G., Schlitzer, R., Slater, R., Swathi, P., Totterdell, I., Weirig, M., Yamanaka, Y., Yool, A., and Orr, J.: Evaluation of ocean carbon cycle models with data-based metrics, *Geophys. Res. Lett.*, 31, L07303, [doi:doi:10.1029/2003GL018970](https://doi.org/10.1029/2003GL018970), 2004.
- McDermott, F.: Palaeo-climate reconstruction from stable isotope variations in speleothems: a review, *Quaternary Sci. Rev.*, 23, 901–918, [doi:doi:10.1016/j.quascirev.2003.06.021](https://doi.org/10.1016/j.quascirev.2003.06.021), 2004.
- 715 McNeil, B. I., Matear, R. J., and Tilbrock, B.: Does carbon 13 track anthropogenic CO₂ in the Southern Ocean?, *Global Biogeochem. Cy.*, 15, 597–613, 2001.
- Meissner, K. J.: Younger Dryas: a data to model comparison to constrain the strength of the overturning circulation, *Geophys. Res. Lett.*, 34, L21705, [doi:doi:10.1029/2007GL031304](https://doi.org/10.1029/2007GL031304), 2007.
- 720 Meissner, K. J., Schmittner, A., Weaver, A. J., and Adkins, J. F.: Ventilation of the North Atlantic Ocean during the Last Glacial Maximum: a comparison between simulated and observed radiocarbon ages, *Paleoceanography*, 18, 1023, [doi:doi:10.1029/2002PA000762](https://doi.org/10.1029/2002PA000762), 2003.
- Mook, W. G.: ¹³C in atmospheric CO₂, *Neth. J. Sea Res.*, 20, 211–223, 1986.
- Moore, J. K., Lindsay, K., Doney, S. C., Long, M. C., and Misumi, K.: Marine ecosystem dynamics and biogeochemical cycling in the Community Earth System Model [CESM1(BGC)]: comparison
- 725 of the 1990s with the 2090s under the RCP4.5 and RCP8.5 scenarios, *J. Climate*, 26, 9291–9312, [doi:doi:10.1175/JCLI-D-12-00566.1](https://doi.org/10.1175/JCLI-D-12-00566.1), 2013.
- Naegler, T.: Reconciliation of excess ¹⁴C-constrained global CO₂ piston velocity estimates, *Tellus B*, 61, 372–384, 2009.

- 730 Naegler, T. and Levin, I.: Closing the global radiocarbon budget 1945–2005, *J. Geophys. Res.*, 111, D12311, [doi:doi:10.1029/2005JD006758](https://doi.org/10.1029/2005JD006758), 2006.
- Naegler, T., Ciais, P., Rodgers, K., and Levin, I.: Excess radiocarbon constraints on air–sea gas exchange and the uptake of CO₂ by the oceans, *Geophys. Res. Lett.*, 33, L11802, [doi:doi:10.1029/2005GL025408](https://doi.org/10.1029/2005GL025408), 2006.
- NCL Version 6.2.0, Boulder, C. U.: The NCAR Command Language, [doi:doi:10.5065/D6WD3XH5](https://doi.org/10.5065/D6WD3XH5), 2014.
- 735 O’Leary, M. H.: Measurement of the isotope fractionation associated with diffusion of carbon dioxide in aqueous solution, *J. Phys. Chem.*, 88, 823–825, 1984.
- Orr, J. C.: Global Ocean Storage of Anthropogenic Carbon (GOSAC), Tech. rep., EC Environment and Climate Program, Final Report, 2002.
- Orr, J., Najjar, R., Sabine, C., and Joos, F.: Abiotic-HOWTO, Technical report, revision: 1.16, available at: <http://ocmip5.ipsl.jussieu.fr/OCMIP/phase2/simulations/Abiotic/HOWTO-Abiotic.html> (last access: 15 May 2012), 2000.
- 740 Peacock, S.: Debate over the ocean bomb radiocarbon sink: closing the gap, *Global Biogeochem. Cy.*, 18, GB2022, [doi:doi:10.1029/2003GB002211](https://doi.org/10.1029/2003GB002211), 2004.
- Petit, J. R., Jouzel, J., Raynaud, D., Barkov, N. I., Barnola, J.-M., Basile, I., Bender, M., Chappellaz, J., Davis, M., G, D., Delmotte, M., Kotlyakov, V. M., Legrand, M., Lipenkov, V. Y., Lorius, C., Pepin, L., Ritz, C., Saltzman, E., and Stievenard, M.: Climate and atmospheric history of the past 420,000 years from the Vostok ice core, Antarctica, *Nature*, 399, 429–436, 1999.
- 745 Polka, J. S., van Beynenb, P., Asmeromc, Y., and Polyakc, V. J.: Reconstructing past climates using carbon isotopes from fulvic acids in cave sediments, *Chem. Geol.*, 360–361, 1–9, [doi:doi:10.1016/j.chemgeo.2013.09.022](https://doi.org/10.1016/j.chemgeo.2013.09.022), 2013.
- Popp, B. N., Laws, E. A., Ridigare, R. R., Dore, J. E., Hanson, K. L., and Wakeham, S. G.: Effect of phytoplankton cell geometry on carbon isotope fractionation, *Geochim. Cosmochim. Ac.*, 62, 69–77, 1998.
- Quay, P. D., Tilbrook, B., and Wong, C. S.: Oceanic uptake of fossil fuel CO₂: carbon-13 evidence, *Science*, 256, 74–79, 1992.
- 755 Rau, G. H., Takahashi, T., and Marais, D. J. D.: Latitudinal variations in plankton δ¹³C: implications for CO₂ and productivity in past oceans, *Nature*, 341, 516–518, 1989.
- Raymond, P. A., Bauerb, J. E., Caracoc, N. F., Colec, J. J., Longworthd, B., and Petschd, S. T.: Controls on the variability of organic matter and dissolved inorganic carbon ages in northeast US rivers, *Mar. Chem.*, 92, 353–366, 2004.
- 760 Schmittner, A., Gruber, N., Mix, A. C., Key, R. M., Tagliabue, A., and Westberry, T. K.: Biology and air–sea gas exchange controls on the distribution of carbon isotope ratios (δ¹³C) in the ocean, *Biogeosciences*, 10, 5793–5816, [doi:doi:10.5194/bg-10-5793-2013](https://doi.org/10.5194/bg-10-5793-2013), 2013.
- Shields, C. A., Bailey, D. A., Danabasoglu, G., Jochum, M., Kiehl, J. T., Levis, S., and Park, S.: The low-resolution CCSM4, *J. Climate*, 25, 3993–4014, [doi:doi:10.1175/JCLI-D-11-00260.1](https://doi.org/10.1175/JCLI-D-11-00260.1), 2012.
- 765 Sikes, C. S., Roer, R. D., and Wilbur, K. M.: Photosynthesis and coccolith formation: inorganic carbon sources and net inorganic reaction of deposition, *Limnol. Oceanogr.*, 25, 248–261, 1980.
- Soetaert, K., Herman, P. M. J., and Middelburg, J. J.: A model of early diagenetic processes from the shelf to abyssal depths, *Geochim. Cosmochim. Ac.*, 60, 1019–1040, [doi:doi:10.1016/0016-7037\(96\)00013-0](https://doi.org/10.1016/0016-7037(96)00013-0), 1996.
- Sonnerup, R. E., Quay, P. D., McNichol, A. P., Bullister, J. L., Westby, T. A., and Anderson, H. L.: Reconstruct-

Table 1. Parameters ~~using~~used in the parameterization of ϵ_p for the implementation following Keller and Morel (1999). The values for small phytoplankton are based on *E. huxleyi*, the value for diatoms are based on *P. tricornutum*, and the values for diatoms are based on ~~based on~~Synechococcus sp. (Keller and Morel, 1999; Popp et al., 1998).

	Small phytoplankton	Diatom	Diazotroph
Qc [mol C cell ⁻¹]	69.2×10^{-14}	63.3×10^{-14}	3×10^{-14}
cell _{permea} [ms ⁻¹]	1.8×10^{-5}	3.3×10^{-5}	3.0×10^{-8}
cell _{surf} [m ²]	87.6×10^{-12}	100.6×10^{-12}	5.8×10^{-12}
C _{up}	2.2	2.3	7.5
ϵ_{fix}	25.3	26.6	30

- 770 ing the ocean ¹³C Suess effect, Global Biogeochem. Cy., 13, 857–872, [doi:doi:10.1029/1999GB900027](https://doi.org/10.1029/1999GB900027), 1999.
- Stuiver, M. and Polach, H. A.: Discussion: reporting of ¹⁴C Data, Radiocarbon, 19, 355–363, 1977.
- Sweeney, C., Gloor, E., Jacobson, A. R., Key, R. M., McKinley, G., Sarmiento, J. L., and Wanninkhof, R.: Constraining global air–sea gas exchange for CO₂ with recent bomb ¹⁴C measurements, Global Biogeochem. Cy., 21, GB2015, [doi:doi:10.1029/2006GB002784](https://doi.org/10.1029/2006GB002784), 2007.
- 775 Tagliabue, A. and Bopp, L.: Towards understanding global variability in ocean carbon-13, Global Biogeochem. Cy., 22, GB1025, [doi:doi:10.1029/2007GB003037](https://doi.org/10.1029/2007GB003037), 2008.
- Toggweiler, J. R., Dixon, K., and Bryan, K.: Simulations of radiocarbon in a coarse-resolution world ocean model 1. Steady state prebomb distributions, J. Geophys. Res., 94, 8217–8242
- 780 [doi:doi:10.1029/JC094iC06p08217](https://doi.org/10.1029/JC094iC06p08217), 1989.
- Tortell, P. D., Reinfelder, J. R., and More, F. M. M.: Active uptake ~~of~~of bicarbonate by diatoms, Nature, 390, 243–244, 1997.
- Turner, J. V.: Kinetic fractionation of ¹³C during calcium carbonate precipitation, Geochim. Cosmochim. Ac., 46, 1183–1191, [doi:doi:10.1016/0016-7037\(82\)90004-7](https://doi.org/10.1016/0016-7037(82)90004-7), 1982.
- 785 Wanninkhof, R.: Relationship between wind speed and gas exchange over the ocean, J. Geophys. Res., 97, 7373–7382, 1992.
- Waugh, D. W., Hall, T. M., and Haine, T. W. N.: Relationships among tracer ages, J. Geophys. Res., 108, 3138, [doi:doi:10.1029/2002JC001325](https://doi.org/10.1029/2002JC001325), 2003.
- Yellowstone: Computational and Information Systems Laboratory, National Center for Atmospheric Research,
- 790 Boulder, CO, Yellowstone: IBM iDataPlex System (Climate Simulation Laboratory), available at: <http://n2t.net/ark:/85065/d7wd3xhc> (last access: 15 September 2014), 2012.
- Zeebe, R. E. and Wolf-Gladrow, D.: CO₂ in Seawater: Equilibrium, Kinetic, Isotopes, 3rd Edn., Elsevier Oceanography Series 65, Elsevier Ltd, 2001.
- Zhang, J., Quay, P. D., and Wilbur, D. O.: Carbon isotope fractionation during gas–water exchange and dissolution of CO₂, Geochim. Cosmochim. Ac., 59, 107–114, 1995.
- 795 Ziveri, P., Stoll, H. M., Probert, I., Klaas, C., Geisen, M., J., J. Y., and Ganssen, G.: Stable isotope vital effects in coccolith calcite, Earth Planet. Sc. Lett., 210, 137–149, 2003.

Table 2. Excess oceanic radiocarbon inventory, measured in 10^{26} atoms of ^{14}C , from various sources for 1975 (GEOSECS) and 1995 (WOCE). Corrections by Naegler et al. (2006) are for neglected ocean regions, corrections by Naegler (2009) are for neglected contributions from increasing DIC. The values from this study are listed at the bottom, for the abiotic and biotic implementation. The biotic excess radiocarbon inventories are the same for all biological fractionation choices tested.

Publication	1975 (GEOSECS)	1995 (WOCE)
Broecker et al. (1980)	314 ± 35	
Broecker et al. (1985)	289	
Lassey et al. (1990)	303	
Hesshaimer et al. (1994)	225	
Broecker and Peng (1994)	300	
Broecker et al. (1995)	305 ± 30	
Peacock (2004) multitracer correlation	241 ± 60	335 ± 15
corrected by Naegler et al. (2006)	245 ± 60	340 ± 15
corrected by Naegler (2009)	252 ± 60	367 ± 15
Peacock (2004) silicate approach	262 ± 26	
corrected by Naegler et al. (2006)	264 ± 26	
Key et al. (2004)		313 ± 47
corrected by Naegler et al. (2006)		355 ± 50
corrected by Naegler (2009)		383 ± 50
Naegler and Levin (2006)	258 ± 13	367 ± 17
Sweeney et al. (2007)	225	343 ± 40
corrected by Naegler (2009)	232	370 ± 40
Naegler (2009)		373 ± 98
This study, abiotic ^{14}C	286 <u>297</u>	372 <u>389</u>
This study, biotic ^{14}C	291 <u>295</u>	384 <u>390</u>

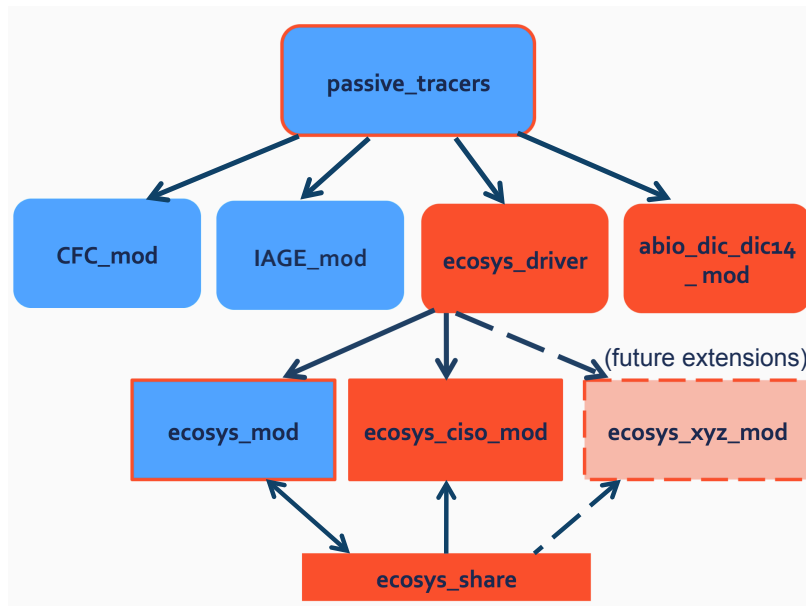


Fig. 1. Schematic of the passive tracer modules with the new ecosystem driver and carbon isotope modules. Existing modules are shown in blue, new modules are shown in red, and edited modules are shown in blue with a red box. Dashed lines indicate future developments. This schematic shows how the ecosystem driver acts as an interface between the ecosystem-related modules and the passive tracers module that drives all tracer modules as well as how *ecosys_share* is used to share variables computed by the ecosystem model and used by other modules beside the ecosystem model.

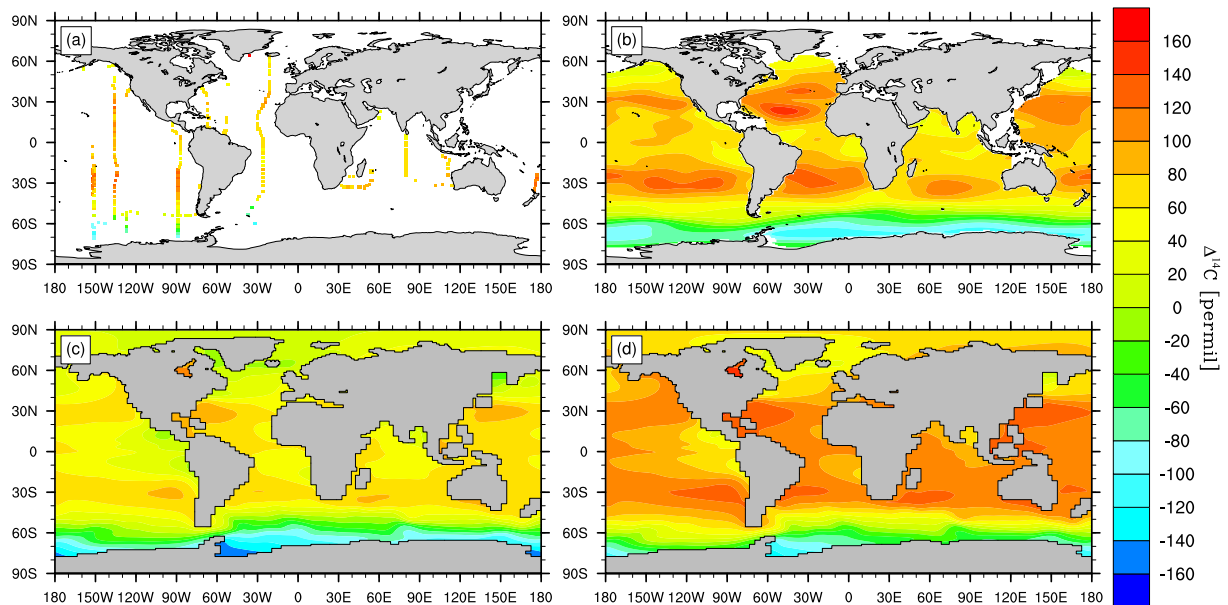


Fig. 2. Surface values of total $\Delta^{14}\text{C}$ from the 1990s (including bomb ^{14}C) from (a) cruise data compiled by Schmittner et al. (2013), (b) the gridded GLODAP data (Key et al., 2004), (c) simulated biotic $\Delta^{14}\text{C}$, and (d) simulated abiotic $\Delta^{14}\text{C}$.

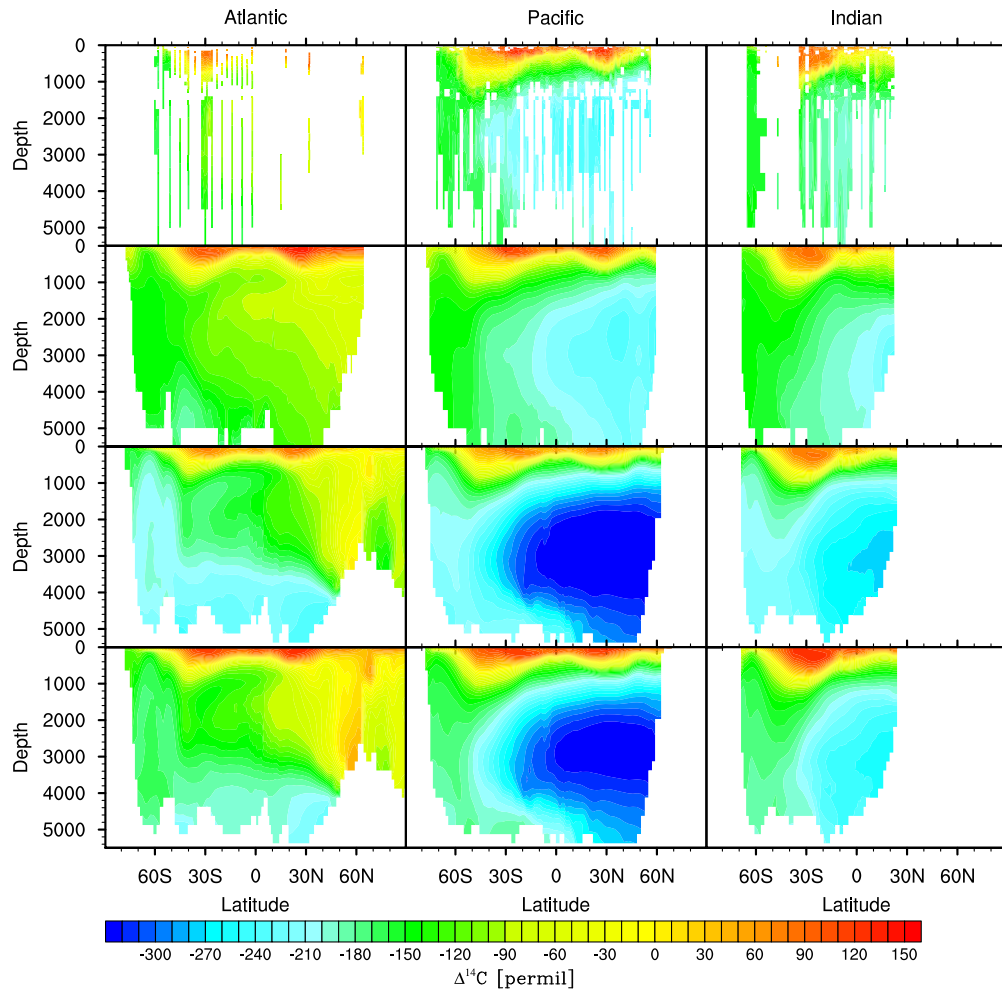


Fig. 3. Zonal averages of total $\Delta^{14}\text{C}$ for the Atlantic, Pacific, and Indian Ocean for the 1990s, from cruise data compiled by Schmittner et al. (2013) (top row), the gridded GLODAP data (Key et al., 2004) (second row), the $\Delta^{14}\text{C}$ from the biotic model (third row), and the abiotic model (bottom row). Note that due to the sparse observational data (see Fig. 2a for the coverage at the surface), the zonal average from the cruise data in the top row is more of a zonal composite than a zonal average.

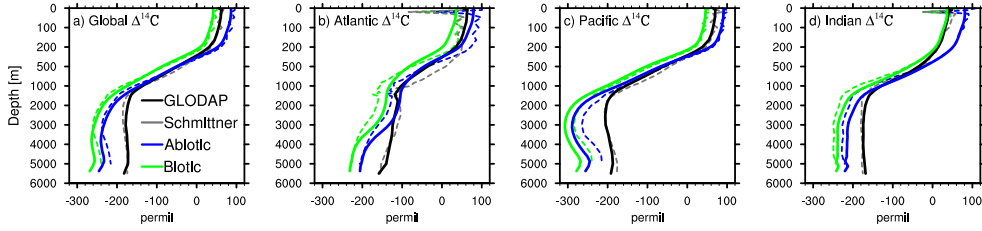


Fig. 4. Depth profiles of $\Delta^{14}\text{C}$ for (a) the global ocean, (b) the Atlantic Ocean, (c) the Pacific Ocean, and (d) the Indian Ocean. The simulated biotic (green) and abiotic (blue) $\Delta^{14}\text{C}$ is compared to the global gridded GLODAP $\Delta^{14}\text{C}$ (black) dataset (Key et al., 2004). In addition dashed lines show the cruise data compiled by Schmittner et al. (2013) (gray) and the model simulated data subsampled at the same locations as this data (green and blue dashed lines).

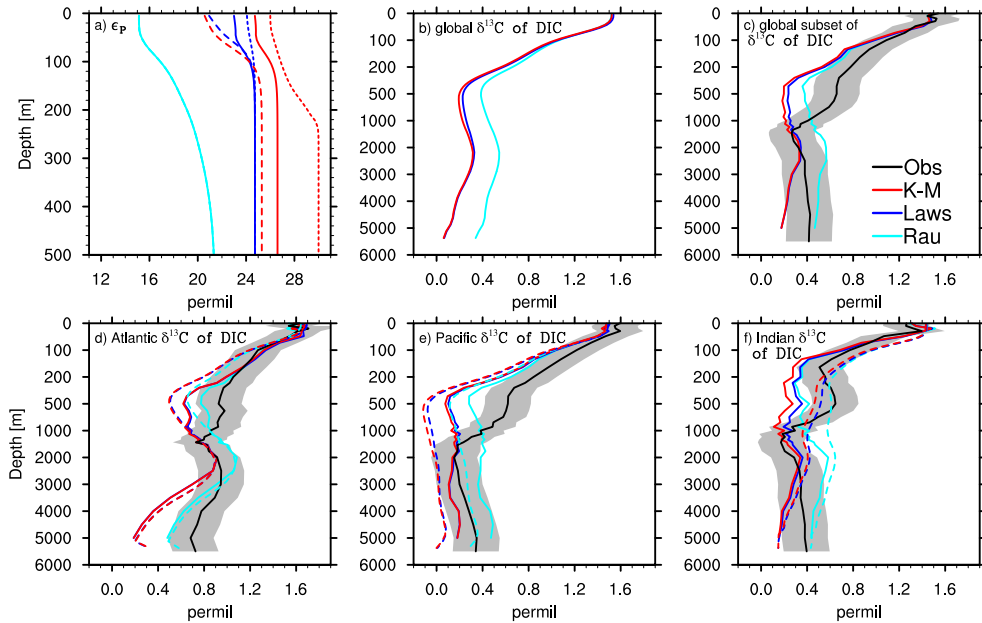


Fig. 5. (a) Depth profiles over the top 500 m (where ϵ_p is important because of primary production) of the globally-averaged values of ϵ_p produced by the three tested parameterizations for biological fractionation for diatoms (solid line), diazotrophs (short dashes), and small phytoplankton (large dashes). The simulated globally-averaged depth profile (0–6000 m) of $\delta^{13}\text{C}_{\text{DIC}}$ in the 1990s is shown in (b), and the global average depth profile of the subset model $\delta^{13}\text{C}_{\text{DIC}}$ for the same grid points as in the cruise data compiled by Schmittner et al. (2013) is shown in (c). Basin average depth-profiles are shown in (d–f), with dashed lines showing the full basin average from the model and solid lines showing the subset averages for the same points as the cruise data compiled by Schmittner et al. (2013). The uncertainty for the cruise data is shown as grey shading in (c), and is $\pm 0.2\%$ (Schmittner et al., 2013). Note that the irregular y axis in (b–f) emphasizes the upper ocean.

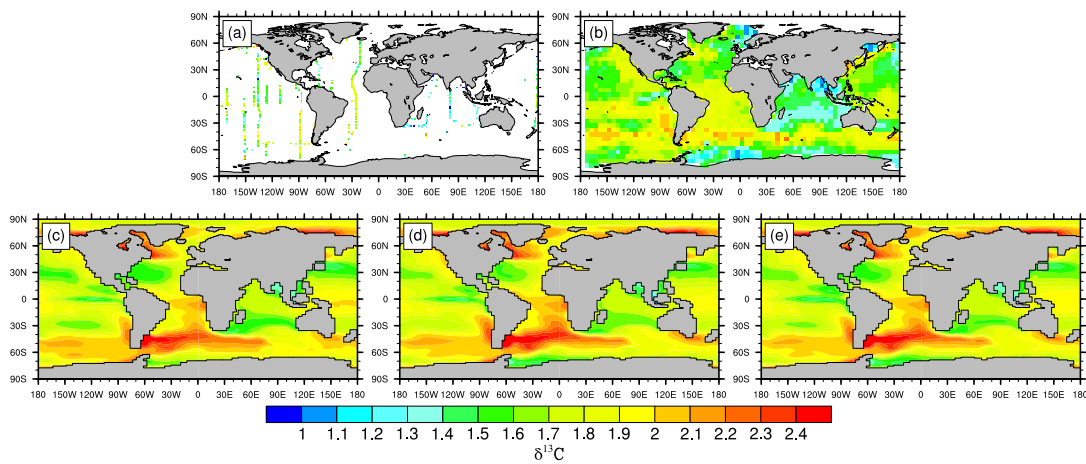


Fig. 6. Surface values of $\delta^{13}\text{C}$ for the 1990s from (a) cruise data compiled by Schmittner et al. (2013), (b) 5° extrapolated gridded data from Gruber and Keeling (1999) and Gruber and Keeling (2001), and (c–e) the biotic model, using the biological fractionation from (c) Rau et al. (1989), (d) Laws et al. (1995), and (e) Keller and Morel (1999).

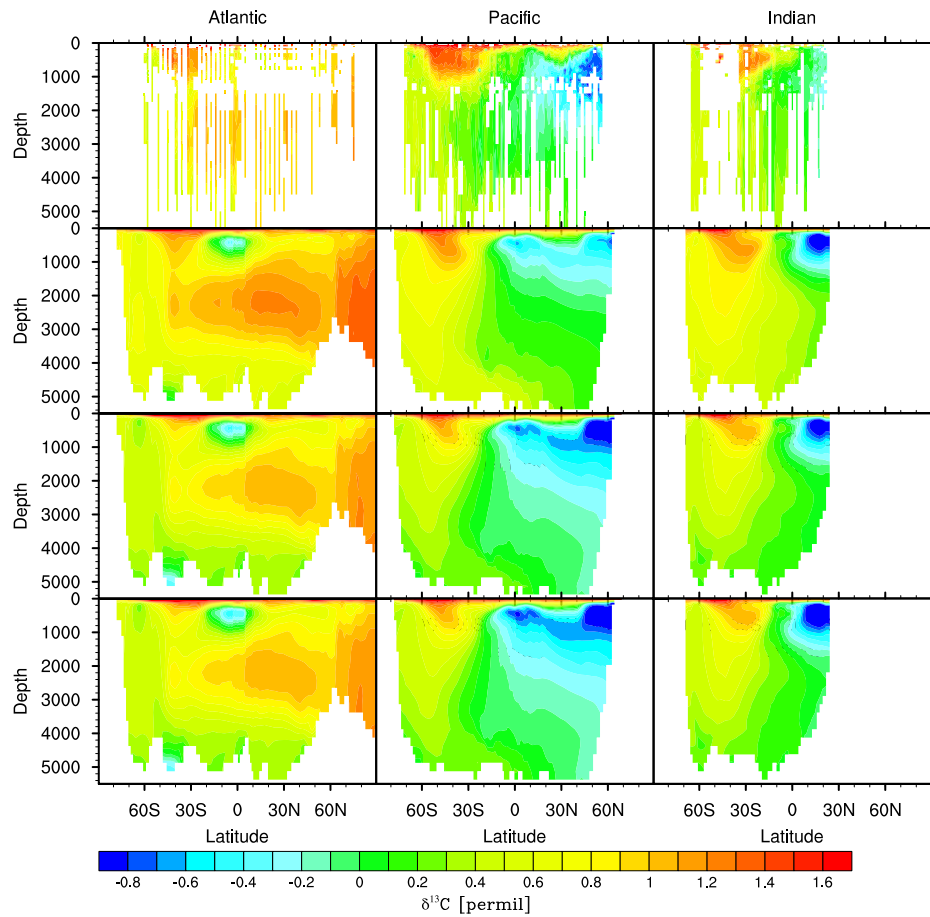


Fig. 7. Zonal ocean basin composites from the cruises data compiled by Schmittner et al. (2013) (top row), compared to 1990s zonal basin averages from the model simulation using the biological fractionation from Rau et al. (1989) (second row), Laws et al. (1995) (third row), and Keller and Morel (1999) (bottom row).

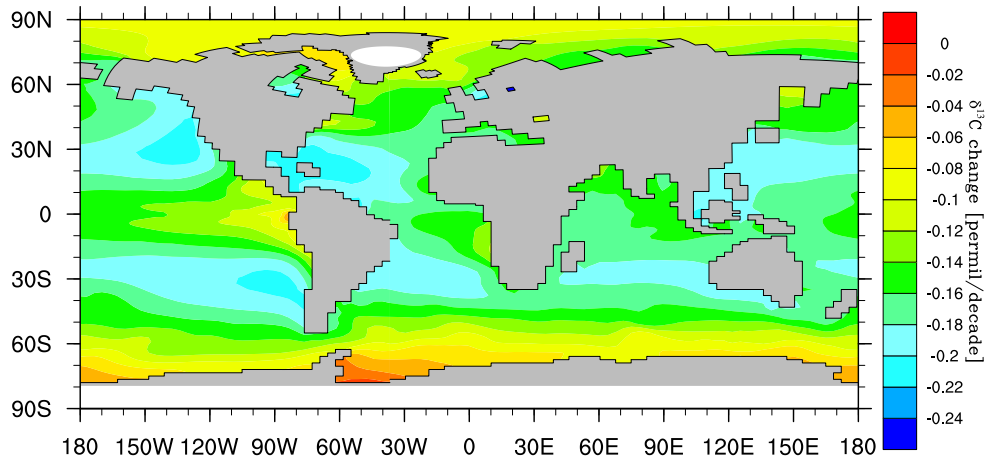


Fig. 8. Surface ocean Suess effect (the change in $\delta^{13}\text{C}$) between 1970 and 1990, in ‰ decade^{-1} .